CAPITAL UNIVERSITY OF SCIENCE AND
TECHNOLOGY, ISLAMABAD

Stability Analysis and Newton Basin of Attraction for a Test Mass in the Isosceles Trapezoid Central Configuration

by

Shehar Bano

A thesis submitted in partial fulfillment for the
degree of Master of Philosophy

in the

Faculty of Computing
Department of Mathematics

2024

Copyright © 2024 by Shehar Bano

All rights reserved. No part of this thesis may be reproduced, distributed, or transmitted in any form or by any means, including photocopying, recording, or other electronic or mechanical methods, by any information storage and retrieval system without the prior written permission of the author.

Dedicated to My Parents

CERTIFICATE OF APPROVAL

Stability Analysis and Newton Basin of Attraction for a Test Mass in the Isosceles Trapezoid Central Configuration

by

Shehar Bano

Registration No: MMT213032

THESIS EXAMINING COMMITTEE

S. No.	Examiner	Name	Organization
(a)	External Examiner	Dr. Tooba Feroze	NUST, Islamabad
(b)	Internal Examiner	Dr. Rashid Ali	CUST, Islamabad
(c)	Supervisor	Dr. Abdul Rehman Kashif	CUST, Islamabad

Supervisor Name
Dr. Abdul Rehman Kashif
July, 2024

Dr. Muhammad Sagheer
Head
Dept.of Mathematics
July, 2024

Dr. M. Abdul Qadir
Dean
Faculty of Computing
July, 2024

Author's Declaration

I, **Shehar Bano** hereby state that my MPhil thesis titled "**Stability Analysis and Newton Basin of Attraction for a Test Mass in the Isosceles Trapezoid Central Configuration**" is my own work and has not been submitted previously by me for taking any degree from Capital University of Science and Technology, Islamabad or anywhere else in the country/abroad.

At any time if my statement is found to be incorrect even after my graduation, the University has the right to withdraw my MPhil Degree.

(Shehar Bano)

Registration No: MMT213032

Plagiarism Undertaking

I solemnly declare that research work presented in this thesis titled "**Stability Analysis and Newton Basin of Attraction for a Test Mass in the Isosceles Trapezoid Central Configuration**" is solely my research work with no significant contribution from any other person. Small contribution/help wherever taken has been duly acknowledged and that complete thesis has been written by me.

I understand the zero tolerance policy of the HEC and Capital University of Science and Technology towards plagiarism. Therefore, I as an author of the above titled thesis declare that no portion of my thesis has been plagiarized and any material used as reference is properly referred/cited.

I undertake that if I am found guilty of any formal plagiarism in the above titled thesis even after award of MPhil Degree, the University reserves the right to withdraw/revoke my MPhil degree and that HEC and the University have the right to publish my name on the HEC/University website on which names of students are placed who submitted plagiarized work.

(Shehar Bano)

Registration No: MMT213032

Acknowledgement

This thesis becomes a reality with the kind support and help of many individuals. I would like to extend my sincere thanks to all of them. Foremost, I want to offer this endeavor to **Almighty Allah** for the wisdom he bestowed upon me, the strength, peace of my mind and good health in order to finish this research thesis.

My sincere gratitude goes out to **Dr. Abdul Rehman Kashif**, my supervisor, whose unwavering support and insightful feedback were invaluable to my success in completing this project. Thanks to his wisdom, kind assistance, and insightful critiques, I was able to complete my thesis.

I will always be grateful to **my parents**, my **parents in law** and my **husband** for their prayers and tireless support. I am eternally grateful for the unending love and encouragement they have given me throughout my life.

I wish to express my appreciation to my friends especially **Saman Israr**, **Seher Urooj**, **Habiba Ghaffar** and **Saliha Ameen** for their inspiration, assistance, and direction to complete my thesis. And last but not least I am very thankful to **Mr. Atif Ali Zafar** for his time and sincerely appreciate the assistance.

(Shehar Bano)

Registration No: MMT213032

Abstract

This thesis proposes a method to identify central configurations in the general coplanar four-body problem with four distinct masses. By introducing a restricted body, the problem transitions to a restricted five-body scenario. In this setup, three masses form a triangle's vertices, while the fourth mass can be positioned elsewhere on the plane, forming either convex or concave central configurations. We establish the necessary conditions for central configurations and ensure the masses are positive. We use analytical and numerical approaches to delineate regions where central configurations are feasible. Specifically, examine the four point masses arranged at the vertices of an isosceles trapezoid with two pairs of equal masses. We analyze the motion of a fifth negligible mass without impacting the primary four masses dynamics. We determine equilibrium positions within a specified interval $(0.5, 1)$ for the restricted fifth body. Additionally, we investigate the Newton basins of attraction relative to these equilibrium points.

Contents

List of Figures

List of Tables

Abbreviations

2BP	Two Body Problem
3BP	Three Body Problem
4BP	Four Body Problem
CC	Central Configuration
M_s	Mass of the Sun
$R5BP$	restricted five-body problem

Symbols

G	Universal Gravitational Constant	$m^3kg^{-1}s^{-2}$
F	Gravitational Force	Newton
s	Distance	m
P	Linear Momentum	$kgms^{-1}$
L	Angular Momentum	kgm^2s^{-1}
m_i	point masses	kg
$\wedge$	Cross Product	

Chapter 1

Introduction

1.1 Background

A Central Configuration (CC) denotes a distinctive alignment of point masses, governed by Newton's law of gravitation, characterized by the condition that the gravitational acceleration vector acting on each mass, due to all others, directs towards the center of mass and is directly proportional to the distance from the center of mass. CCs hold significant significance in examining the Newtonian n- body problem. They are crucial because they produce the only explicit solutions to the equations of motion, control the trajectory patterns near collisions, and influence the structural arrangement of integral manifolds.
About 67% of the stars in our galaxy are estimated to belong to multistellar systems, underscoring the significance of comprehending both the four-body problem and the five-body problem. CCs serve as valuable tools for understanding gravitational challenges in systems with multiple bodies.

In 1998 Steves and Roy studied the specific symmetric four-body problem where in around an axis two pairs of equal masses were arranged symmetrically, successfully determined indirect analytical central configurations. They identified central configurations, including the trapezoid, four collinear, the diamond convex kite and two triangular concave kites. Interestingly, it was demonstrated that these configurations ultimately reduced to Lagrangian solutions when a pair of masses had their mass approach zero, essentially

converging to the limit of the CRTBP [1]. Additionally, Shoaib (2004) further detailed the triangular concave kite central configurations.

Subsequently, numerous authors including Meyer and Schmidt (2005)[2], Albouy, Fu et al. (2008) [3], Waldvogel (2012)[4], Erdi et al. (2016) [5], Shoaib et al. (2017) [6] have delved into the exploration of central configurations in the four-body problem. They employed various symmetry constraints to address this challenging problem.

Notably, Roberts et al. (2018) [7] demonstrated that every convex arrangement of four bodies, where the diagonals of the quadrilateral are perpendicular, always takes on the form of a kite. Erdi et al. (2016) extended their investigation to encompass a more generalized problem with a single axis of symmetry. Erdi et al. introduced angular coordinates, substantially simplifying the process of deducing central configurations for both concave and convex scenarios in the four-body problem (4BP) [5].

Furthermore,in 2019 Alvarez and Llibre effectively obtained central configurations for Hjelmslev quadrilaterals as well as for Equilic quadrilaterals [8].

P´erez-Chavela and Santoprete (2007), Mello and Fernandes (2011) [9], Waldvogel (2012)[4] and Yan (2012) delved into the study of the kite Four Body Problem(4BP). Llibre et al. (2009) explored a 4BP characterized by three equal masses, demonstrating the precise count of central configurations for kites [10].

Santroprete in 2018, examined a four body problem featuring one pair of parallel sides. Utilizing distances as their variables, Santroprete established the existence of kites central configurations and isosceles trapezoids[11]. Celli (2007)[12] and Llibre and Corbera (2014) [13] also addressed the topic of central configurations involving trapezoids.

Xia (2004) offered a straightforward proof for the well-known result from Bartky and MacMillan (1932)[14]. Corbera et al. (2019) [15] extensively explored various trapezoidal configurations, encompassing isosceles, acute, and right trapezoids. They carefully examined the symmetry within trapezoidal configurations and uncovered the existence of non-symmetrical trapezoidal configurations.

Roberts and Cors (2012) [16] delved into co-circular trapezoidal central configurations and demonstrated that a line of symmetry emerges when two masses are of equal magnitude within cocircular four-body central configurations [17]. In addition to their study of quadrilaterals, isosceles trapezoidal configurations also investigated by Bartky and MacMillan(1932) [18].

For a considerable time period central configurations in the co-planar n -body problem have been a widely known phenomenon. These configurations represent unique equilibrium solutions where a system of n bodies, each with mass m_i, revolves around their center of mass at a fixed angular velocity. The geometric arrangement resulting from this motion remains unaltered, and the central configuration exhibits remarkable stability under transformations such as scaling, translation, rotation, and reflection, while preserving its shape.

Prominent and widely recognized instances include the five Lagrange equilibrium solutions in the Circular Restricted Three Body Problem (CRTBP), which give rise to three central configurations of three bodies positioned along a straight line at the L_1, L_2, and L_3 Lagrange points. Additionally, central configurations of two equilateral triangle stem from the L_4 and L_5 Lagrange points.
In the n-body problem of equal masses, central configurations are observed, where n bodies of equal mass are positioned at the vertices of a regular n-gon with sides of equal-length.

Furthermore, it has been known for a considerable time that straight-line collinear solutions exist for n bodies of equal mass [19]. The central configurations for the equal mass four-body problem were found to include the square, isosceles triangle concave kite, four collinear arrangements and the equilateral triangle concave kite.
Moving to scenarios involving problems of non-equal masses, the calculation of central configurations becomes an algebraic but challenging task when n is greater than or equal to 4. In 1978, Simo considering arbitrary masses for all four bodies demonstrated the existence of relative equilibrium solutions in the broader context of the four-body problem. Furthermore, for a restricted four-body problem Simo derived a central configurations which involved three masses and a separate particle [20].

Researchers have extensively examined the stability of central configurations (CC) using both numerical and analytical methods, as demonstrated by Bakker and Simmons [21] and Yan [22]. This analysis offers valuable insights into periodic orbits, stability, and refinement points within the broader context of n-body and four-body problems 4BP. In a News and Reviews article in Nature [23] that reviews advancements in 4BP CC, Hamilton [24] emphasized the potential significance of symmetrical four-body CC. He suggested that these configurations could serve as boundary cases for ambitious future

expansions of the n-body problem. For example, symmetrical configurations might provide insights into scenarios such as three masses aligned on a line with two symmetrically placed equal masses, configurations involving a test particle with planar arrangements similar to those studied in this work, or even planar setups featuring four masses of different magnitudes.

This perspective highlights the ongoing exploration and potential applications of symmetrical four-body CC in advancing our understanding of celestial dynamics. These findings could serve as foundational scenarios for ambitious expansions of the n-body problem, including cases with three aligned masses and two equal masses symmetrically positioned, a test particle with planar configurations akin to those in this study, or planar arrangements with four distinct masses.

1.2 Newton's Basins of Attraction

The Newton-Raphson iterative method leverages inherent characteristics of dynamic systems to identify the convergence areas linked with Lagrange points. Various literature delves into these convergence areas tied to Lagrange points across diverse dynamic systems, including the restricted three-body problem [25]. Suraj et al. and colleagues conducted a recent exploration on the analysis of restricted five-body problem within frame of variable mass, examining the positional dynamics and stability of a Lagrange point concerning a perturbation parameter influenced by the variable mass of a fifth, diminutive body [26].

They applied an iterative Newton-Raphson bivariate approach to explore convergence areas for equilibrium points. These attraction zones is illustrate how the system's of equilibrium points draw in initial conditions, and they are positioned as nodes on the configuration plane, constituting a domain of convergence.

The discussion revolved around Newton-Raphson convergence basins linked to Lagrange points, which serve as attractors, within the planar circular restricted 5-body problem [27]. Bogdan and collaborators explored fractal attraction basins linked to the damped Newton method [28]. Suraj et al. conducted recent numerical studies on the constrained five-body problems in a concave axisymmetric configuration. They utilized the iterative Newton-Raphson method to identify basin convergence [29].

Consider a restricted five-body problem(R5BP), where four positive masses, forming two pairs of equal masses situated at neighboring vertices by fixing on some position, move in a manner ensuring their configuration remains that of an isosceles trapezoid. Concurrently, a smaller mass denoted as m_5 moves within the same plane, subject to the gravitational pull exerted by the four primaries, without affecting the motion of these four primaries. Calculate the coordinates of equilibrium points, and determine the basins of attraction according to Newton's laws.

1.3 Outline of Thesis

The thesis is structured into five chapters as follows:

- **Chapter 1**

  In this chapter Introduction, a literature review of centeral configuration and Newton's basin of attraction is provided.

- **Chapter 2**

  In Chapter 2 some basic definitions and laws of celestial mechanics, including Newton's laws of motion, Newton's universal law of gravitation and Kepler's laws of planetary motion are provided. Additionally, it discusses the 2BP and the n-BPs.

- **Chapter 3**

  In this chapter, a comprehensive review of the paper referenced as [30] is provided.

- **Chapter 4**

  In Chapter 4, The equation of motion for 5^{th} body is used to find out the equilibrium points of R5BP and then plotted the Newton Basins of attraction for these equilibrium points.

- **Chapter 5**

  This chapter concludes the study, give summarizing insights and concluding remarks.

- **The bibliography** contains references cited throughout the thesis.

Chapter 2

Preliminaries

This section encompasses crucial definitions and regulatory statutes that are essential for comprehending the content presented in the following next chapter. [31–36].

2.1 Basic Defination

2.1.1 Newtonian Mechanics

Newtonian mechanics is a mathematical structure aimed at elucidating the motion of diverse entities within the cosmos. Initially articulated by Sir Isaac Newton in his renowned work, Philosophiae Naturalis Principia Mathematica (Mathematical Principles of Natural Philosophy), commonly referred to as the Principia, first published in 1687.

2.1.2 Celestial Mechanics [37]

"Celestial Mechanics is devoted to the study of the motion of the celestial bodies which influence each other, mainly due to the gravitational law. This discipline has born and developed together with humankind."

2.1.3 Degree of Freedom [31]

"The number of coordinates required to specify the position of a system of one or more particles is called number of degree of freedom of the system. Example: A particle moving freely in space requires 3 coordinates (x, y, z), to specify its position. Thus the number of degree of freedom is 3."

2.1.4 Scalar [31]

"Various quantities of physics, such as length, mass and time, requires for their specification a single real number such quantities are called scalars and the real number is called the magnitude of the quantity."

e.g. mass, time, volume, density and temperature.

2.1.5 Vector [31]

"Some quantities of physics, such as displacement, velocity, momentum, force etc require for their specification a direction as well as magnitude, Such quantities are called vectors."

e.g. displacement, velocity, acceleration, force and weight

2.1.6 Field [31]

"A field is a physical quantity associated with every point of space-time. The physical quantity may be either in vector form, scalar form or tensor form."

2.1.7 Vector Field [31]

"If at every point in a region, a vector function has a defined value, the region is called a vector field.

Mathematically,

$$f = \mathbb{R}^3 \to \mathbb{R}^3$$

e.g. tangent vector around a smooth curve."

2.1.8 Scalar Field [31]

"If at every point in a region, a scalar function has a defined value, the region is called a scalar field.
e.g. temperature and pressure fields around the earth."

2.1.9 Conservative Vector Field [31]

"A vector field $\mathbf{V}$ is conservative if and only if there exists a continuously differentiable scalar field 'f' such that $\mathbf{V} = -\nabla f$ or equivalently if and only if

$$\nabla \times \mathbf{V} = Curl\, \mathbf{V} = 0."$$

2.1.10 Uniform Force Field [31]

"A force field $\mathbf{F}$ which has constant magnitude and direction is called a uniform or constant force field. If the direction of the field is taken as negative z direction and magnitude is constant $F_0 > 0$, then the force field is given by

$$\mathbf{F} = -F_0\hat{\mathbf{k}}."$$

2.1.11 Central Force [31]

"Suppose that a force acting on a particle of mass m such that

(a) it is always directed from m toward or away from a fixed point O,

(b) its magnitude depends only on the distance r from origin. Then we call the force a central force or central force field with O as the center of force. In symbols $\mathbf{F}$ is a central force if and only if

$$\mathbf{F} = f(r)\hat{r}$$

where $\hat{r}$ is a unit vector in the direction of position vector $\mathbf{r}$. The central force is one of attraction towards O or repulsion from O according as $f(r) < 0$ or $f(r) > 0$ respectively."

2.1.12 Center of Mass [31]

"Let $\mathbf{r}_1, \mathbf{r}_2, ..., \mathbf{r}_n$ be the position vector of a system of n particles of masses $m_1, m_2, ...m_n$ respectively. The center of mass or centroid of the system of particles is defined as that point having position vector.

$$\begin{aligned}\hat{\mathbf{r}} &= \frac{m_1\mathbf{r}_1 + m_2\mathbf{r}_2 + ... + m_n\mathbf{r}_n}{m_1 + m_2 + ... + m_n}, \\ &= \frac{1}{\mathbf{M}}\sum_{v=1}^{n} m_v\mathbf{r}_v,\end{aligned}$$

where

$$\mathbf{M} = \sum_{v=1}^{n} m_v,$$

is the total mass of the system."

2.1.13 Torque [32]

"The torque is a vector quantity that measures the tendency of that force to rotate the particle about O and is defined as

$$\boldsymbol{\tau} = \mathbf{r} \times \mathbf{F}.$$

The direction of $\boldsymbol{\tau}$ is perpendicular to the plane formed by $\mathbf{r}$ and $\mathbf{F}$. From the vector product definition, this quantity has a magnitude given by

$$\tau = rF\sin\theta.$$

where θ is the smaller angle between $\mathbf{r}$ and $\mathbf{F}$, $\boldsymbol{\tau}$ is positive if the force tends to rotate the particle counterclockwise and negative if it tends to rotate it clockwise."

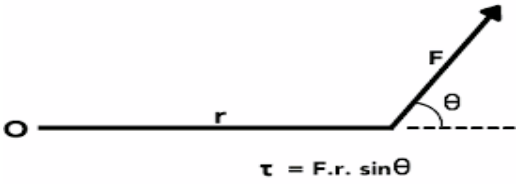

FIGURE 2.1: Torque of a system

2.1.14 Momentum [32]

"The linear momentum of a particle of mass m is a vector quantity defined as

$$\mathbf{p} = m\mathbf{v}.$$

where $\mathbf{v}$ is the velocity of the particle. A fast moving car has more momentum than a slow moving car of the same mass. Newton's second law can be expressed in terms of momentum for a particle-like object of constant mass as

$$\sum \mathbf{F} = m\mathbf{a} = m\frac{d\mathbf{v}}{dt} = \frac{d(m\mathbf{v})}{dt} = \frac{d\mathbf{p}}{dt},$$

so the rate of change of the linear momentum of an object is equal to the resultant force acting on the object and is in the same direction as that of force."

2.1.15 Angular Momentum [32]

"The angular momentum $\mathbf{L}$ of a particle of mass m is a vector quantity defined as:

$$\mathbf{L} = \mathbf{r} \times \mathbf{p},$$

where $\mathbf{r}$ is the position vector of the particle relative to an origin O that is in an inertial frame.

2.1.16 Conservation of Angular Momentum [32]

"The total angular momentum of a particle is constant if the net external torque acting on it is zero:

$$\sum \boldsymbol{\tau_{ext}} = \frac{d\mathbf{L}}{dt} = 0,$$

$$\mathbf{L} = C,$$

where C is a constant vector then,

$$\mathbf{L}_i = \mathbf{L}_f."$$

2.1.17 Central Configuration [36]

"A central configuration is a special arrangement of point masses interacting by Newton's law of gravitation with the following property: the gravitational acceleration vector produced on each mass by all the others should point toward the center of mass and be proportional to the distance to the center of mass."

2.1.18 Zero Velocity Surfaces

Zero velocity surfaces or curves act as constraints preventing a satellite or any object moving under the gravitational pull of larger bodies from crossing them. These regions delineate the allowed and restricted zones of motion for the satellite. Take, for instance, the well-known "Restricted Three-Body Problem," involving two primary masses and a much smaller third particle affected b y t heir g ravitational p ull b ut m oving independently.
Introducing a centrifugal force through a rotating coordinate system with stationary masses alters the conservation of energy and momentum. While energy and momentum aren't conserved independently in this system, the Jacobi integral remains constant, represented by the equation $v^2 = 2U - C$, where v denotes the velocity of the smaller particle, U signifies the effective potential, and C represents the Jacobi constant, named after Carl Jacobi, a German mathematician who discovered it in 1836.

This constant, also known as the constant of motion for the smaller particle, ensures v^2 cannot be negative. The zero velocity surfaces are determined by $2U - C = 0$, and the permissible motion regions for the particle are identified by $2U - C > 0$ to prevent negative values for v^2.

2.2 Frame of Reference [31]

" A particle can be at rest or in uniform motion in a straight line with respect to one frame of reference and be traveling in a curve and accelerating with respect to another frame of reference.

If Newton's laws hold in one frame of reference they also hold in any other frame of reference which is moving at constant velocity relative to it. All such frames of

reference are called inertial frames of reference or Newtonian frames of reference.

To all observers in such inertial systems the force acting on a particle will be the same, i.e. it will be invariant."

2.3 Newton's Law of Motion [32]

"The following three laws of motion given by Sir Isaac Newton are considered axioms of mechanics:.

2.3.1 Newton's First Law of Motion [32]

Every particle persists in a state of rest or of uniform motion in a straight line (Le. with constant velocity) unless acted upon by a force.

2.3.2 Newton's Second Law of Motion [32]

If $\mathbf{F}$ is the (external) force acting on a particle of mass m which as a consequence is

moving with velocity $\mathbf{v}$, then $\mathbf{F} = (mv)$ where $p = mv$ is momentum. If the mass

m does not very with time t this become $F = m\frac{dp}{dt} = m\mathbf{a}$,

2.3.3 Newton's Third Law of Motion [32]

To every action, there is an equal and opposite reaction."

2.4 Kepler's Law of Planetary Motion [32]

"Kepler's three laws of planetary motion can be described as follows:

2.4.1 Kepler's First Law(The Law of Orbit) [32]

Every planet moves in an orbit which is an ellipse, with the Sun at one focus.

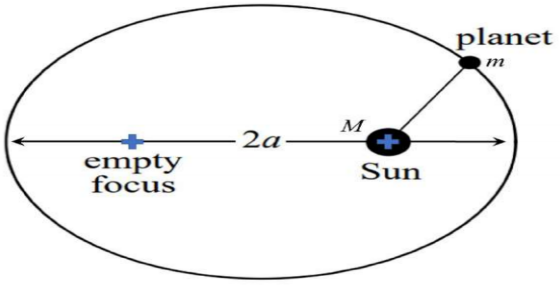

FIGURE 2.2: In the geometric representation of Kepler's first law, the Sun occupies one of the two focal points of the planet's elliptical orbit, while the other focal point remains unoccupied.

2.4.2 Kepler's Second Law(The Law of Areas) [32]

The radius vector drawn from the sun to any planet sweeps out equal areas in the equal time."

2.4.3 Kepler's Third Law(The Law of Periods) [32]

"The square of the periods of revolution of the planets are proportional to the cubes of semi-major axis of the their orbits. Mathematically, Kepler's third law can be written as:

$$T^2 = \left(\frac{4\pi^2}{GM_s}\right)a^3,$$

where T is the time period, a is the semi major axis, M_s is the mass of sun and G is the universal gravitational constant.

2.5 Newton's Universal Law of Gravitation [31]

Any two particles of masses m_1 and m_2 espectively and distancer apart are attracted toward each other with a force

$$\mathbf{F} = G\frac{m_1 m_2}{r^3}\mathbf{r},$$

where G is universal gravitational constant. Its numerical value in SI units is $6.67408 \times 10^{-11} m^3 kg^{-1} s^{-2}$."

2.6 Two Body Problem [33]

"The two-body problem is a simplified scenario in which two point masses interact only through their gravitational attraction. In this problem, the motion of one mass (a planet) is influenced by the gravitational force exerted by another mass. If at a specific time t the positions and velocities of two known masses affected by their mutual gravitational interaction then their position and velocities can be find at any other time."

2.6.1 The Solution of Two Body Problem [34]

"Newton's law of universal gravitation, provided the mathematical framework for solving the two-body problem.

$$\mathbf{F} = G\frac{mM}{s^3}\mathbf{s}. \tag{2.1}$$

Considering two masses, m and M, with a separation of distance s and governed by the universal gravitational constant G. The objective is to determine the trajectory of the particles over a period of time t, assuming their initial positions and velocities are known. The attractive force, $\mathbf{F_{12}}$, between these masses is oriented towards m_1 along the $\mathbf{s}$ direction, while the force, $\mathbf{F_{21}}$, acting on M is directed in the opposite direction.

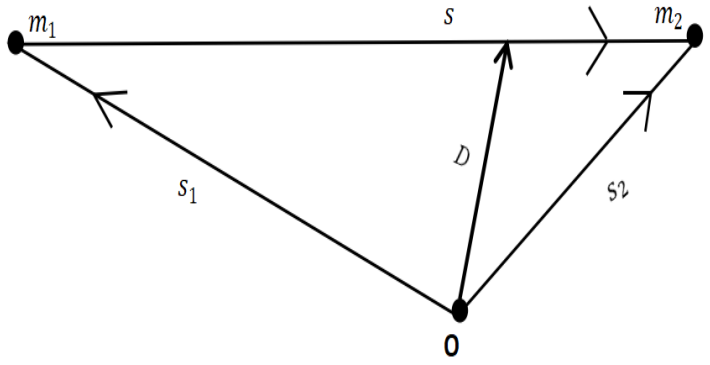

FIGURE 2.3: Center of mass

In accordance with the third law of motion proposed by Newton,

$$\mathbf{F_{12}} = -\mathbf{F_{21}}, \tag{2.2}$$

where

$$\mathbf{F_{12}} = G\frac{mM}{d^3}\mathbf{s}, \tag{2.3}$$

$$\mathbf{F_{21}} = G\frac{mM}{d^3}\mathbf{s}, \tag{2.4}$$

The equations describing the motion of particles influenced by their gravitational interactions are provided through equations (2.1) and (2.2) by applying Newton's second law of motion.

$$m\ddot{\mathbf{s_1}} = G\frac{m_1 m_2}{s^3}\mathbf{s}, \tag{2.5}$$

$$m\ddot{\mathbf{s_2}} = -G\frac{m_1 m_2}{s^3}\mathbf{s}. \tag{2.6}$$

The position vectors s_1 and s_2 are measured from the reference point O, as depicted in Figure 2.3. Upon applying equations (2.4) and (2.5), we obtain

$$m_1\ddot{\mathbf{s_1}} + m_2\ddot{\mathbf{s_2}} = \mathbf{0}. \tag{2.7}$$

Integrating the above equations results in below equation and that will be total linear momentum of the system which is constant.

$$m_1\dot{\mathbf{s_1}} + m_2\dot{\mathbf{s_2}} = \mathbf{h}, \tag{2.8}$$

Again integrating the above equation, we get

$$m_1\mathbf{s_1} + m_2\mathbf{s_2} = h\mathbf{t} + g. \tag{2.9}$$

where h and g are the constant of integration.

According to the definition of the center of mass provided by 2BPs

$$m_t\mathbf{D} = m_1\mathbf{s_1} + m_2\mathbf{s_2}, \tag{2.10}$$

where $\mathbf{D}$ is the center of mass and m_t is sum of masses m_1 and m_2. Firstly,

By differen-tiating the equation (2.9) and then compare with equation (2.7.)

$$m_t\dot{\mathbf{D}} = \mathbf{k_1} \implies \dot{\mathbf{s}} = \frac{\mathbf{k_1}}{m_t} = Constant. \tag{2.11}$$

show that the velocity of center of mass is constant. Taking equation (2.5) and subtracting equation (2.6) results in:

$$\ddot{\mathbf{s_1}} - \ddot{\mathbf{s_2}} = G\frac{m_2}{s^3}\mathbf{s} + G\frac{m_1}{s^3}\mathbf{s}, \tag{2.12}$$

$$\ddot{\mathbf{s_1}} - \ddot{\mathbf{s_2}} = G(m_2 + m_1)\frac{\mathbf{s}}{s^3}, \tag{2.13}$$

$$\ddot{\mathbf{s}} = \beta\frac{\mathbf{s}}{s^3}, \tag{2.14}$$

$$\implies \ddot{\mathbf{s}} + \beta\frac{\mathbf{s}}{s^3} = 0. \tag{2.15}$$

Here, the reduced mass, denoted as β, is defined as $\beta = G(m_1 + m_2)$, and the difference between $\mathbf{s_1} - \mathbf{s_2}$ is represented as $\mathbf{s}$. Now multiply $\mathbf{s}$ with equation (2.14)

$$\mathbf{s}\ddot{\mathbf{s}} + \frac{s^3}{\mathbf{s}} \times \mathbf{s} = 0 \tag{2.16}$$

$$\implies \mathbf{s} \times \ddot{\mathbf{s}} = 0, \tag{2.17}$$

Upon integration of the equation mentioned above, it transforms into:

$$\mathbf{s} \times \dot{\mathbf{s}} = \mathbf{H}, \tag{2.18}$$

where $\mathbf{H}$ is an integration constant. Equation (2.15) becomes

$$\mathbf{s} \times \beta\ddot{s} = 0, \tag{2.19}$$

$$\mathbf{s} \times \mathbf{F} = 0, \tag{2.20}$$

$$\mathbf{F} = \beta\ddot{\mathbf{s}}. \tag{2.21}$$

The concepts of torque and angular momentum are taken from chapter 2

$$\boldsymbol{\tau} = \frac{d\mathbf{H}}{dt} = \mathbf{s} \times \mathbf{F}.$$

After comparison

$$\boldsymbol{\tau} = \frac{d\mathbf{H}}{dt} = \mathbf{s} \times \mathbf{F} = 0,$$

$$\frac{d\mathbf{H}}{dt} = 0,$$
$$\mathbf{H} = Constant.$$

This suggests that angular momentum remains unchanged or is preserved."

2.7 Radial and Transverse Components of Velocity and Acceleration

If we select polar coordinates s and θ within this depicted region, the velocity components along and perpendicular to the radius vector connecting m_1 and m_2 are represented as $\dot{s}$ and $s\dot{\theta}$.

$$v = \dot{\mathbf{s}} = \dot{s}\hat{i} + s\dot{\theta}\hat{j}, \tag{2.22}$$

where v is the velocity of particle in polar coordinate and unit vectors $\hat{i}$ and $\hat{j}$ are positioned parallel and perpendicular to the radius vector. Taking cross product with $s\hat{i}$,

$$s\hat{i} \times (\dot{s}\hat{i} + s\dot{\theta}\hat{j}) = s^2\dot{\theta}\hat{k} = L\hat{k}, \tag{2.23}$$

the unit vector $\hat{k}$ is orthogonal or perpendicular to the orbital plane. We can write,

$$s^2\dot{\theta} = L, \tag{2.24}$$

since L remains constant and is demonstrated to be twice the rate of change of the radius vector, this provides a mathematical representation of Kepler's second law.

From figure(2.3) we know that

$$\dot{\mathbf{s_1}} - \dot{\mathbf{s_2}} = -\dot{\mathbf{s}}$$

so we can write equation as

$$\frac{s^2(-\dot{\mathbf{s}})}{st^2} = G\frac{m_1 m_2}{s^3}\mathbf{s}$$

where $G(m_1 + m_2)$ are constant so,

$$\frac{d^2(\dot{\mathbf{s}})}{dt^2} + \beta\frac{\mathbf{s}}{s^3}\mathbf{s} = 0, \tag{2.25}$$

If we take the dot product of $\dot{\mathbf{s}}$ with equation (2.25) we derive the following equations, as shown below.

$$\dot{\mathbf{s}} \cdot \frac{d^2\mathbf{s}}{dt^2} + \beta\frac{\dot{\mathbf{s}} \cdot \mathbf{s}}{s^3} = 0.$$

After integrating the above equation we get,

$$\frac{1}{2}\dot{\mathbf{s}} \cdot \dot{\mathbf{s}} - \frac{\beta}{s} = H, \tag{2.26}$$

$$\frac{1}{2}v^2 - \frac{\beta}{s} = H. \tag{2.27}$$

The constant H represents energy conservation in this system. It's important to note that H does not represent the absolute energy; instead, $\frac{1}{2}v^2$ corresponds to kinetic energy (KE), and $\frac{-\beta}{s}$ corresponds to potential energy (PE) of the system. This means that the total energy of the system remains constant. When considering the elements of the acceleration vector in celestial mechanics, the radius vector is both perpendicular to and aligned along certain directions.

Taking the derivative of equation (2.22), the acceleration vector is given as follows

$$\mathbf{a} = (\ddot{s} - s\dot{\theta}^2)\hat{i} + \frac{1}{s}\frac{s}{st}(s^2\theta)\hat{j}, \tag{2.28}$$

above equation is used in equation (2.25), we obtain,

$$\ddot{s} - s\dot{\theta}^2 = -\frac{\beta}{s^2}, \tag{2.29}$$

$$\frac{1}{s}\frac{s}{st}(s^2\dot{\theta}) = 0. \tag{2.30}$$

Following further integration of equation (2.30), we arrive at the subsequent integral for angular momentum.

$$s^2\dot{\theta} = L. \tag{2.31}$$

With this type of substitution,

$$u = \frac{1}{s}, \tag{2.32}$$

by using equation (2.32) in central force we get:

$$\frac{s^2 u}{s\theta^2} + u = \frac{\beta}{L^2}, \tag{2.33}$$

the equation above exhibits a familiar shape, which is:

$$u = \frac{\beta}{L^2} + B\cos(\theta - \theta_0), \tag{2.34}$$

in the given equation, substitute $u = \frac{1}{s}$, where B and θ_0 are integration constants.

$$\frac{1}{s} = \frac{\beta}{L^2} + B\cos(\theta - \theta_0), \tag{2.35}$$

$$s = \frac{\frac{\beta}{L^2}}{1 + \frac{L^2 B_1}{\beta}\cos(\theta - \theta_0)},$$

the polar form of the conical equation can be expressed as:

$$s = \frac{p}{1 + \epsilon\cos(\theta - \theta_0)},$$

where

$$p = \frac{L^2}{\beta},$$

$$\epsilon = \frac{BL^2}{\beta}.$$

The trajectory of one celestial body as it revolves around another is characterized by the eccentricity (ϵ) of the orbit, and it can be classified as follows:

1. If $0 < \epsilon < 1$, then the orbit will be elliptical.

2. If $\epsilon = 1$ then the orbit iwill be parabolic.

3. Similarly, the orbit will be hyperbolic when ϵ exceeds 1.

Therefore, Kepler's first law is a particular instance of the conic section that represents the solution to the 2BP.

2.8 Restricted Three Body Problem

The restricted three-body problem is a classical problem in physics and celestial mechanics that deals with the motion of three bodies under the influence of gravity, where one body is significantly less massive than the other two. In this problem, it is assumed that the mass of the smaller body is negligible compared to the masses of the other two bodies, and thus its gravitational influence on the other bodies can be ignored.

Chapter 3

Central configuration equations for four body co-planar masses

In this chapter we review the work of Shoaib et.al [30].

3.1 The Mathematical Expression Representing Central Configuration

"We consider the case of four positive point masses m_i having position vectors s_i and inter-body distances s_{ij}, $i, j = 0, 1, 2, 3$. The masses are co-planar but not collinear. The equations for a non-collinear central configuration can be written

$$f_{ij} = \sum_{k=0, k\neq i,j}^{n-1} m_k(R_{ik} - R_{jk})\nabla_{ijk} = 0, \tag{3.1}$$

where $R_{ij} = s_{ij}^{-3}$ and $\delta_{ijk} = (s_i - s_j) \wedge (s_i - s_k)$ and δ represent the triangle area which are determined by $(s_i - s_j)(s_i - s_k)$ [38]".

When a central configuration is subjected to scaling, translation, rotation, or reflection, the resulting system remains a central configuration. Assuming that no mass aligns, start by choosing a mass, denoted as m_1, and position it at $s_1 = (-1, 0)$. Then, choose two other masses m_0 and m_2, and rotate the entire system in such a way that the line connecting

m_0 and m_2 becomes perpendicular to the x-axis. While preserving the orientation and the fixed position of m_1, scale the entire system until m_0 and m_2 are positioned along the y-axis. If needed, and without compromising generality, across the x-axis perform a reflection of the system so that m_0 is located at $s_0 = (0, b)$ and m_2 is positioned at $s_2 = (0, a)$, where $b < a$. We record the final body's coordinates m_3, to be $s_3 = (d_1, d_2)$.

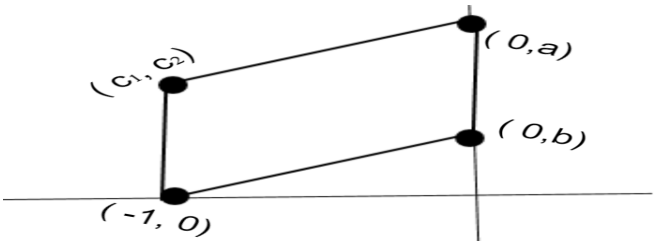

FIGURE 3.1: Position of Primary Masses

We can now express R_{ij} and δ_{ijk} as follows:

$$\left.\begin{aligned} R_{01} = \frac{1}{\Phi}, \quad R_{02} = \frac{1}{\Psi}, \quad R_{12} = \frac{1}{\Upsilon}, \\ R_{03} = \frac{1}{T}, \quad R_{13} = \frac{1}{X}, \quad R_{23} = \frac{1}{Z}. \end{aligned}\right\} \tag{3.2}$$

$$\left.\begin{aligned} \delta_{012} = b - a, \qquad \delta_{013} = b + bd_1 - d_2, \\ \delta_{023} = (b-a)d_1, \quad \delta_{123} = d_2 - a - ad_1, \end{aligned}\right\} \tag{3.3}$$

where

$$\Upsilon = (1+a^2)^{\frac{3}{2}}, \Phi = (1+b^2)^{\frac{3}{2}}, \Psi = (a-b)^3$$

$$Z = (d_1^2 + (d_2 - a)^2)^{\frac{3}{2}}, T = (d_1^2 + (d_2 - b)^2)^{\frac{3}{2}}, X = (d_2^2 + (d_1 + 1)^2)^{\frac{3}{2}}$$

Note that

$$\delta_{ijk} = \delta_{kij} = \delta_{jki} = -\delta_{kji} = -\delta_{jik} = -\delta_{ikj},$$

and if $j = k$, $k = i$, $j = i$ then $\delta_{ijk} = 0$.

Let

$$\omega_0 = \frac{m_0}{m_3}, \ \omega_1 = \frac{m_1}{m_3}, \ \omega_2 = \frac{m_2}{m_3}. \tag{3.4}$$

Upon substituting the expressions from equations (3.2), (3.3), and (3.4), equation (3.1) transforms into the following form:

$$\left.\begin{aligned}
f_{01} &= \omega_2(b-a)\left(\frac{1}{\Psi}-\frac{1}{\Upsilon}\right)+\left(\frac{1}{\Upsilon}-\frac{1}{X}\right)(b+bd_1-d_2)=0,\\
f_{02} &= \omega_1\left(\frac{1}{\Phi}-\frac{1}{\Upsilon}\right)-\left(\frac{1}{T}-\frac{1}{Z}\right)d_1=0,\\
f_{03} &= \omega_1\left(\frac{1}{\Phi}-\frac{1}{X}\right)(d_2-b-bd_1)-\omega_2(b-a)\left(\frac{1}{\Psi}-\frac{1}{Z}\right)d_1,\\
f_{12} &= \omega_0(b-a)\left(\frac{1}{\Phi}-\frac{1}{\Psi}\right)+\left(\frac{1}{X}-\frac{1}{Z}\right)(d_2-a-ad_1)=0,\\
f_{13} &= \omega_0\left(\frac{1}{\Phi}-\frac{1}{T}\right)(d_2-b-bd_1)+\omega_2\left(\frac{1}{\Upsilon}-\frac{1}{Z}\right)(d_2-a-ad_1)=0,\\
f_{23} &= \omega_0(a-b)\left(\frac{1}{\Psi}-\frac{1}{T}\right)d_1-\omega_1\left(\frac{1}{\Upsilon}-\frac{1}{X}\right)(d_2-a-ad_1)=0.
\end{aligned}\right\} \tag{3.5}$$

By selecting these coordinates, it becomes possible with fixed values for a, b, d_1, and d_2 to achieve any planar non-collinear four-body geometric configuration .

3.2 Conditions for the Presence of Central Configurations Involving Four Bodies

Theorem.3.1

Consider a problem with four masses m_0, m_1, m_2 and m_3 and position vectors $s_0 = (0,b)$, $s_1 = (1,0)$, $s_2 = (0, a)$, $s_3 = (d_1, d_2)$, where $a, b, d_1, d_2 \in \mathbf{R}$ with $a > 0$, $b \neq a$, and $\Upsilon \neq \Phi$, $\Psi \neq \Upsilon$, $\Psi \neq \Phi$.

In order for $r = (s_0,\ s_1,\ s_2,\ s_3)$ to be a central configuration, specific mass ratios must exist uniquely.

$$\omega_0 = \frac{(d_2-a-ad_1)(X-Z)\Phi\Psi}{(a-b)(\Phi-\Psi)XZ}, \tag{3.6}$$

$$\omega_1 = \frac{d_1(Z-T)\Upsilon\Phi}{(\Upsilon-\Phi)ZT}, \tag{3.7}$$

$$\omega_2 = \frac{(d_2-b-bd_1)(X-T)\Upsilon\Psi}{(a-b)(\Psi-\Upsilon)XQ}, \tag{3.8}$$

subject to the constraint

$$V(a,b,d_1,d_2) = \Psi(\Upsilon-\Phi)X + T((\Psi-\Upsilon)X + \Upsilon(\Phi-\Psi)) + Z((\Upsilon-\Phi)T + (\Phi-\Psi)X + \Phi(\Psi-\Upsilon)) = 0, \tag{3.9}$$

where Υ, Φ, Ψ, X, T and Z are provided with in equations (3.2).

proof:

Suppose $\Phi \neq \Psi \neq \Upsilon$, then solving $f_{12}=0$, $f_{02}=0$ and $f_{01}=0$ of equations (3.5) for ω_0, ω_1 and ω_2 respectively and simplifying the corresponding expressions we obtain equations (3.6). Substituting the expressions of ω_0, ω_1 and ω_2 into $f_{03}=0$, $f_{13}=0$ and $f_{23}=0$ of equations (3.5), we get

$$d_1(d_2-b-bd_1)V_1(a,b,d_1,d_2) = 0, \tag{3.10}$$

$$(d_2-a-ad_1)(d_2-b-bd_1)V_2(a,b,d_1,d_2) = 0, \tag{3.11}$$

$$d_1(d_2-a-ad_1)V_3(a,b,d_1,d_2) = 0, \tag{3.12}$$

where

$$v_1(a,b,d_1,d_2) = \frac{\left(\frac{1}{T}-\frac{1}{Z}\right)\left(\frac{1}{\Phi}-\frac{1}{X}\right)}{\left(\frac{1}{\Phi}-\frac{1}{\Upsilon}\right)} - \frac{\left(\frac{1}{T}-\frac{1}{X}\right)\left(\frac{1}{\Psi}-\frac{1}{Z}\right)}{\left(\frac{1}{\Psi}-\frac{1}{\Upsilon}\right)}, \tag{3.13}$$

$$v_2(a,b,d_1,d_2) = \frac{\left(\frac{1}{X}-\frac{1}{Z}\right)\left(\frac{1}{\Phi}-\frac{1}{T}\right)}{\left(\frac{1}{\Phi}-\frac{1}{\Psi}\right)} - \frac{\left(\frac{1}{T}-\frac{1}{X}\right)\left(\frac{1}{\Upsilon}-\frac{1}{Z}\right)}{\left(\frac{1}{\Phi}-\frac{1}{\Upsilon}\right)}, \tag{3.14}$$

$$v_3(a,b,d_1,d_2) = \frac{\left(\frac{1}{T}-\frac{1}{Z}\right)\left(\frac{1}{\Upsilon}-\frac{1}{S}\right)}{\left(\frac{1}{\Phi}-\frac{1}{\Upsilon}\right)} - \frac{\left(\frac{1}{X}-\frac{1}{Z}\right)\left(\frac{1}{\Psi}-\frac{1}{T}\right)}{\left(\frac{1}{\Phi}-\frac{1}{\Psi}\right)}. \tag{3.15}$$

Equations (3.9) be made up of $v_i(a,b,d_1,d_2)=0$, for $i=1,2,3$ and $d_1=0$, $d_2-b-bd_1=0$ and $d_2-a-ad_1=0$ the straight lines. Considering the premises $\Psi \neq \Upsilon$ and $\Psi \neq \Phi$, we will demonstrate that these three lines do not impose any constraints.

Based on the assumption $\Phi \neq \Upsilon$, it is clear that $f_{02}=0$ indicate $d_1 \neq 0$. Similarly, in the case of $\Psi \neq \Upsilon$ and $\Psi \neq \Phi$, $f_{01}=0$ implies $d_2-b-bd_1 \neq 0$ and $f_{12}=0$ implies $d_2-a-ad_1 \neq 0$. Hence,

equations (3.9) simplify to the subsequent three equations

$$\begin{aligned} V_1(a,b,d_1,d_2) &= 0, \\ V_2(a,b,d_1,d_2) &= 0, \\ V_3(a,b,d_1,d_2) &= 0. \end{aligned} \tag{3.16}$$

Simplifying equations (3.14), we get

$$\begin{aligned} \frac{\Upsilon V(a,b,d_1,d_2)}{ZTX(\Upsilon-\Phi)(\Upsilon-\Psi)} &= 0, \\ \frac{\Psi V(a,b,d_1,d_2)}{ZTX(\Phi-\Psi)(\Psi-\Upsilon)} &= 0, \\ \frac{\Phi V(a,b,d_1,d_2)}{ZTX(\Upsilon-\Phi)(\Phi-\Psi)} &= 0, \end{aligned} \tag{3.17}$$

where

$$\begin{aligned} V(a,b,d_1,d_2) = \Psi(\Upsilon-\Phi)M + T((\Psi-\Upsilon)X + \Upsilon(\Phi-\Psi)) \\ + Z((\Upsilon-\Phi)T + (\Phi-\Psi)X + \Phi(\Psi-\Upsilon)). \end{aligned} \tag{3.18}$$

Based on the preceding assumptions, equations (3.15) result in

$$V(a,b,d_1,d_2) = 0. \tag{3.19}$$

Equation (3.17) establishes a prerequisite for the presence of four-body central configurations.

To ensure that these central configurations have significance, it is essential that the mass ratios ω_0, ω_1, and ω_2 are all positive.

3.3 Constraints Arising from the Positivity of All Masses

We establish the subsequent lemmas, which are valuable in examining the positivity of mass ratios and in deriving regions for central configurations where

$m_i > 0$.

Lemma 3.1. *Let* $M = m^{3/2}$ *and* $N = n^{3/2}$ *with* m $m > 0$ *and* $n > 0$.

Then

$$M - N = (m - n)B^{+}_{MN}, \tag{3.20}$$

where the factor $B^{+}_{MN} > 0$ *is given by*

$$B^{+}_{MN} = \frac{M^{2/3} + N^{2/3} + (MN)^{1/3}}{M^{1/3} + N^{1/3}}. \tag{3.21}$$

Proof.

$$\begin{aligned} M - N =& m^{3/2} - n^{3/2} = ((\sqrt{m})^3 - (\sqrt{n})^3), \\ =& (\sqrt{m} - \sqrt{n})(m + n + \sqrt{mn}), \\ =& (m - n)(\frac{m + n + \sqrt{mn}}{\sqrt{m} + \sqrt{n}}), \\ =& (m - n)(\frac{M^{2/3} + N^{2/3} + (MN)^{1/3}}{M^{1/3} + N^{1/3}}). \end{aligned}$$

In the lemma that follows, we transform the non-linear components within the expressions for ω_0, ω_1, *and* ω_2 as presented in equation (6), converting them into products of linear factors involving d_1 and d_2. This transformation facilitates the derivation of analytical expressions for the areas where central configurations exist with positive ratios of masses.

lemma 3.2

The ratios of masses ω_0, ω_1, and ω_2 as specified in equation (3.6), can be expressed in the subsequent format.

$$\omega_0 = \frac{(d_2 - a - ad_1)(2ad_2 + 2d_1 + 1 - a^2)\Phi\Psi B^{+}_{XZ}}{(a - b)(1 - a_2 + 2ab)XZB^{+}_{\Phi\Psi}}, \tag{3.22}$$

$$\omega_1 = \frac{d_1(a + b - 2d_2)\Upsilon\Phi B^{+}_{ZT}}{(a + b)ZTB^{+}_{\Upsilon\Phi}}, \tag{3.23}$$

$$\omega_2 = \frac{(d_2 - b - bd_1)(2bd_2 + 2d_1 + 1 - b^2)\Upsilon\Psi B^{+}_{XT}}{(a - b)(b^2 - 2ab - 1)XTB^{+}_{\Psi\Upsilon}}, \tag{3.24}$$

where $B^{+}_{\cdot}$ is the positive factor defined by 3.19.

proof:

Using lemma (3.1) and equation (3.2) , we obtain the following factorization for $X - Z$ and $\Phi - \psi$.

$$\begin{aligned} X - Z =& (2d_1 + 2ad_2 + 1 - a^2)B^+_{XZ}, \\ \Phi - \Psi =& (1 + b^2 - (a-b)^2)B^+_{\Phi\Psi}. \end{aligned}$$

On substituting the factored form of $Z - X, \Upsilon - \Phi, \Psi - \Upsilon, X - T$ in expression (3.6) , we get the expression for ω_0 , ω_1, ω_2 given in equation (3.21).

$$\begin{aligned} Z - T =& (a-b)(a+b-2d_2B^+_{ZT}), \\ \Upsilon - \Phi =& (a^2 - b^2)B^+_{\Upsilon\Phi}, \\ X - T =& (2d_1 + 2bd_2 + 1 - b^2)B^+_{XT}, \\ \Psi - \Upsilon =& ((a-b)^2 - a^2 - 1). \end{aligned}$$

Equivalent simplified forms, maintaining the same sign as the mass ratios ω_0, ω_1 and ω_2, are provided by the following expressions.

$$\omega_0^* = \frac{(d_2 - a - ad_1)(2ad_2 + 2d_1 + 1 - a^2)}{(a-b)(1 - a_2 + 2ab)}, \tag{3.25}$$

$$\omega_1^* = \frac{d_1(a + b - 2d_2)}{(a+b)}, \tag{3.26}$$

$$\omega_2^* = \frac{(d_2 - b - bd_1)(2bd_2 + 2d_1 + 1 - b^2)}{(a-b)(b^2 - 2ab - 1)}. \tag{3.27}$$

3.4 Determination of Regions of Central Configurations for Positive Mass Ratios

The above lemma 3.2 holds considerable eased the task of pinpointing potential areas for central configurations where all mass ratios are positive.

For example, it's clear that ω_1 is greater than 0 within the specified region.

$$P\omega_1 = \{(a, b, d_1, d_2) | d_2 \in \mathbf{R} \wedge ((b < 2d_2 \wedge ((0 < a < 2d_2 - b \wedge d_1 < 0)$$

$$\vee (a > 2d_2 - b \wedge d_1 > 0))) \vee (b \geq 2d_2 \wedge a > 0 \wedge d_1 > 0))\}. \tag{3.28}$$

Likewise, ω_0 and ω_2 are greater than 0 in the areas S_{ω_0} and S_{ω_2} given below.

$$P_{\omega_0} = \{(a, b, d_1, d_2) | d_2 \in \mathbf{R} \wedge ((\mathcal{A}_2 < -d_2 \wedge ((\mathcal{A}_3 \leq 0 \wedge a > 0 \wedge \mathcal{A}_1 < d_2) \vee (\mathcal{A}_3 > 0$$

$$\wedge((0 < a < \mathcal{A}_3 \wedge \mathcal{A}_1 > d_2) \vee (a > \mathcal{A}_3 \wedge \mathcal{A}_1 < d_2))))) \vee (\mathcal{A}_2 > d_2 \wedge ((\mathcal{A}_3 0 \wedge a > 0 \wedge \mathcal{A}_1 > d_2)$$

$$\vee(\mathcal{A}_3 > 0 \wedge ((0 < a < \mathcal{A}_3 \wedge \mathcal{A}_1 < d_2) \vee (a > \mathcal{A}_3 \wedge \mathcal{A}_1 > d_2))))))\}, \tag{3.29}$$

and

$$S_{\omega_2} = \{(a, b, d_1, d_2) | d_2 \in \mathbf{R} \wedge a > 0 \wedge ((\mathcal{B}_2 < -d_2 \wedge ((\mathcal{B}_3 \leq 0 \wedge ((b < \mathcal{B}_3 \wedge \mathcal{B}_1 > d_2)$$

$$\vee(\mathcal{B}_3 < b < 0 \wedge \mathcal{B}_1 < d_2) \vee (b > 0 \wedge \mathcal{B}_1 > d_2))) \vee (\mathcal{B}_3 > 0 \wedge ((b < 0 \wedge \mathcal{B}_1 > d_2) \vee (0 < b < \mathcal{B}_3$$

$$\wedge \mathcal{B}_1 < d_2) \vee (b > \mathcal{B}_3 \wedge \mathcal{B}_1 > d_2)))) \vee (\mathcal{B}_2 > -d_2 \wedge ((\mathcal{B}_3 \leq 0 \wedge ((b < \mathcal{B}_3 \wedge \mathcal{B}_1 < d_2) \vee (\mathcal{B}_3 < b < 0$$

$$\wedge \mathcal{B}_1 > d_2) \vee (b > 0 \wedge \mathcal{B}_1 < d_2))) \vee (\mathcal{B}_3 > 0 \wedge ((b < 0 \wedge \mathcal{B}_1 < d_2) \vee (0 < b < \mathcal{B}_3 \wedge \mathcal{B}_1 > d_2) \vee (b$$

$$> \mathcal{B}_3 \wedge \mathcal{B}_1 < d_2))))))\}, \tag{3.30}$$

where

$$\mathcal{A}_1 = a + a d_1, \;\; \mathcal{A}_2 = \frac{1 - a^2}{2a} + \frac{d_1}{a}, \;\; \mathcal{A}_3 = b + \sqrt{b^2 + 1},$$

$$\mathcal{B}_1 = b + b d_1, \;\; \mathcal{B}_2 = \frac{1 - b^2}{2b} + \frac{d_1}{b} \quad , \mathcal{B}_3 = -a + \sqrt{a^2 + 1}.$$

The central configuration region in the general four-body problem, under the constraint $\psi(a, b, d_1, d_2) = 0$, is formed by the overlap of the regions P_{ω_0}, P_{ω_1}, and S_{ω_2}. While it's relatively straightforward to identify these central configuration regions for specific mass ratios individually, the process becomes considerably complex when determining their intersection. Moreover, finding the solutions to the geometric constraint $\psi(a, b, d_1, d_2) = 0$ is an even more challenging task and often necessitates the use of computer algebra systems.

3.5 Special Symmetrical Subsets - One Pair of Equal Sides: Isosceles Trapezoid Central Configurations

In this section, we'll investigate a specific scenarios where we treat one pair of sides as having equal lengths and endeavor to identify central configurations for this case. Note that imposing this restriction won't invariably result in the presence of central configurations.

Case 1: $s_{03} = s_{12}$; isosceles trapezoids, equidiagonal kite

The position vector $s_{03} = s_{12}$ by substituting $T = \Upsilon$ in equation(3.6) give

$$\begin{aligned}\omega_0 =& \frac{(d_2 - a - ad_1)(X - Z)\Phi\Psi}{(a-b)(\Phi - \Psi)XZ},\\ \omega_1 =& \frac{d_1(Z - \Upsilon)\Phi}{(\Upsilon - \Phi)Z},\\ \omega_2 =& \frac{(d_2 - b - bd_1)(X - \Upsilon)\psi}{(a-b)(\Psi - \Upsilon)X},\end{aligned} \tag{3.31}$$

and

$$V(a,b,d_1,d_2) = \Upsilon^2(\Phi - \Psi + Z - X) + \Upsilon(2X\Psi - 2\Phi Z) - X\Psi(\Phi + Z) + \Phi Z(\Psi + X), \tag{3.32}$$

where $\Phi \neq \Psi$,$\Upsilon \neq \Phi$,$a \neq b$ and $\Psi \neq \Upsilon$.

It's evident that when X equals Z, Z equals Υ, and X equals Υ, a boundary delineates the regions where the mass ratios ω_0, ω_1, and ω_2 change their sign. In the case presented in this section, ω_0 remains unchanged and retains a positive value as outlined in equation (3.27). The sign of ω_1 is contingent on d_1 and $Z - \Upsilon$. While the sign of ω_2 depends upon $d_2 - b - bd_1$, $X - \Upsilon$, and $\Psi - \Upsilon$.

To obtain the corresponding regions in this specific case, we can make use of expressions (26) and (28) by substituting T with Υ. By setting T equal to Υ, we can reduce one variable and express $V(a, b, d_1, d_2)$ as a function of three variables.
This reduction allows us to numerically solve the equation $V(b, d_1, d_2) = 0$, but finding the intersection with the areas where $\omega_i > 0$ to discover families of central configurations

remains a challenging task. To further simplify the problem, we will introduce a second pair of equal sides.

Case 2: $s_{03} = s_{12}$ and $s_{01} = s_{23}$; isosceles trapezoid

Now consider the case where two pairs of sides are treated as equal, specifically, $s_{03} = s_{12}$ and $s_{01} = s_{23}$ and put $Z = \Phi$. Hinging on the specific values of b, d_1, and d_2, this assumption results in various configurations of quadrilaterals. When we make this assumption, the representaton for ratios of masses and the requisite condition for the presence of a central configuration can be represented as follows:

$$\omega_0 = \frac{(d_2 - a - ad_1)(X - \Phi)\Psi}{(a - b)(\Phi - \Psi)X}, \tag{3.33}$$

$$\omega_1 = -d_1, \tag{3.34}$$

$$\omega_2 = \frac{(d_2 - b - bd_1)(X - \Upsilon)\psi}{(a - b)(\Psi - \Upsilon)X}, \tag{3.35}$$

and the geometric constraint

$$V(a, b) = (X - \Upsilon)(\Psi - \Phi) + (X - \Phi)(\Psi - \Upsilon) = 0. \tag{3.36}$$

The solution obtained when solving both $s_{03} = s_{12}$ and $s_{01} = s_{23}$ simultaneously is:

$$(d_1, d_2) = (1, a + b), (-1, a + b). \tag{3.37}$$

The condition $d_1 = 1$ and $d_2 = a + b$ implies that not only are the two pairs of equal sides, but they are also parallel.

When d_1 takes on this value, it results in $\omega_1 = -1$ for all possible combinations of a and b. This indicates that there are no central configurations with non-negative masses when both pairs of sides are equal and parallel.

Conversely, in the scenario where $d_1 = -1$, we have $\omega_1 = 1$, which is greater than 0, and consequently, m_3 equals m_1. The coordinates of the four masses are now as follows: m_0 at (0, b), m_1 at (-1, 0), m_2 at (0, a), and m_3 at (-1, a + b), which means that s_{13} and s_{02} are parallel to each other.

Lemma 3.3. *The mass ratio ω_0 and ω_2 satisfy ω_0=ω_2.*

Proof. Given that $d_1 = -1$ and $d_2 = a + b$, we can express ω_0 and ω_2 as follows:

$$\omega_0 = \frac{(a+b)\Psi(X-\Phi)}{(a-b)X(\Phi-\Psi)},$$
$$\omega_2 = \frac{(a+b)\Psi(X-\Upsilon)}{(a-b)X(\Psi-\Upsilon)}.$$

The constraint $V(a,b) = 0$ can be written as $\frac{(X-\Phi)}{(\Phi-\Psi)} = \frac{(X-\Upsilon)}{(\Psi-\Upsilon)}$. □

This implies that $\omega_0 = \omega_2$.

To verify the presence of central configurations in cases of non-negative mass ratios, we need to perform a analysis of sign for ω_2 and demonstrate that $V(a,b)$ equals zero.

Lemma 3.4. *Consider the function $V(a,b)$ defined by*

$$V(a,b) = (X-\Upsilon)(\Psi-\Phi) + (X-\Phi)(\Psi-\Upsilon) = 0. \tag{3.38}$$

Then for any $a_0 \in J = (\frac{1}{\sqrt{3}}, 1)$ there exist an open interval $M \subset J$ containing a_0 and an open interval $N \subset (0, \frac{1}{\sqrt{3}})$ containing the solution b_0 of $V(a_0,b_0) = 0$ s.t there exists a unique continuously differentiable function $b = \phi(a)$ defined on M with $b \in N$ that satisfies $V(a,b)$=0.

Proof. For $a < b < a$, the constraint V is defined as follow:

$$V(a,b) = 2(a^3+3ab^2)\ ((1+a^2)^{\frac{3}{2}} + (1+b^2)^{\frac{3}{2}}) - 2(1+a^2)^{\frac{3}{2}}(1+b^2)^{\frac{3}{2}}\ - 2(a^2-b^2)^3. \tag{3.39}$$

Because V exhibits even symmetry with respect to b, it sufficient to examine V for positive values of b. In order to determine the range of values for a, we solve for $w(a,a) = 0$, which provides the lower boundary $a = \frac{1}{\sqrt{3}}$. By solving $V(a,0)$ the upper bound for value of a is found which is 1. It is simple to check that $V(a,0) < 0$ and $V(a, \frac{1}{\sqrt{3}}) > 0$ for

$\frac{1}{\sqrt{3}} < a < 1$. Now we need to show that $\partial V(a,b)/\partial b \neq 0$ for $\frac{1}{\sqrt{3}} < a < 1$ and $0 < b < \dfrac{1}{\sqrt{3}}$. We have

$$\frac{1}{6b}\frac{\partial V(a,b)}{\partial b} = 2a^4 + 2b^4 + 2a(\sqrt{1+a^2} + \sqrt{1+b^4}) + 5ab^2\sqrt{1+b^2}$$
$$+a^3(2\sqrt{1+a^2} + \sqrt{1+b^2}) - 4a^2b^2 - \sqrt{1+a^2}\sqrt{1+b^2} - a^2\sqrt{1+a^2}\sqrt{1+b^2}. \quad (3.40)$$

This resulted in

$$\begin{aligned}\frac{1}{6b}\frac{\partial V(a,b)}{\partial b} &= 2a^4 + 2b^4 + 4a + 5ab^2 + 3a^3 - 4a^2b^2 \\ &\quad - \sqrt{1+a^2}\sqrt{1+b^2} - a^2\sqrt{1+a^2}\sqrt{1+b^2} \\ &\geq 2a^4 + 2b^4 + 4a + ab^2 + 3a^3 - (1+a^2)\sqrt{2}\sqrt{1+a^2} \\ &\geq 2a^4 + 4a + 3a^3 - 2a^2 - 2. \end{aligned} \quad (3.41)$$

For $a \geq \frac{1}{\sqrt{3}}$ the function

$$\phi(a) = 2a^4 + 4a + 3a^3 - 2a^2 - 2$$

is increasing and has minimum $\phi\frac{1}{\sqrt{3}} = \frac{-22}{9} + \frac{5}{\sqrt{3}} > 0$. Hence $\partial V(a,b)/\partial b > 0$. □

In the interval $J = (\dfrac{1}{\sqrt{3}}, 1)$ *let* a_0 *be any number, then* $V(a_0, 0) < 0$ *and* $V(a_0, \frac{1}{\sqrt{3}}) > 0$. *Consequently, By MVT there exist atleast one* $b_0 \in (0, \sqrt{}^{1}_{3})$ *s.t* $V(a_0, b) = 0$. *Due to* $\partial V(a, b)/\partial b \neq 0$ *for all* $a \in J$ *and* $b \in (0, \sqrt{}^{1}_{3})$, *thus is unique. Given that V has continuous partial derivatives and* $V(a_0, b_0) = 0$, *with* $\partial V(a_0, b_0)/\partial b$, *The implicit function theorem implies the existence of an open interval* $M \subset J$ *which contain* $a - 0$ *and an open interval* $N \subset (0, \dfrac{1}{\sqrt{3}})$,*which includes* b_0. *In this context, there is a singular and continuously differentiable function* $b = \phi(a)$ *defined on M such that b N and* $V(a, b) = 0$. *With this, the proof for lemma (3.4) is concluded.*

Now, the sign equivalent expression of ω_2 is given by

$$\omega_2^* = \frac{b^2 + 2ab - 1}{b^2 - 2ab - 1}. \quad (3.42)$$

Due to the zeros of $b^2+2ab-1$ at $a=(b^2-1)/(2b)$ and $b^2-2ab-1ata=(1-b^2)/(2b)$, the regions of central configuration where $\omega_2>0$ are determined given below.

$$R_{\omega 2}=(a,b)\mid(-\frac{1}{\sqrt{3}}<b<0\wedge-b<a<\frac{b^2-1}{2b})\vee(0<b<\frac{1}{\sqrt{3}}\wedge b<a<\frac{1-b^2}{2b}).$$

Therefore, the central configuration area where both pairs of sides in the quadrilateral are equal can be ascertained by examining the overlap between R_{ω_2} and the equation $V(a,b)=0$. This intersection is depicted in Figure 3.1, and the resulting central configuration corresponds to an isosceles trapezoid. In order to acquire quantitative data regarding the

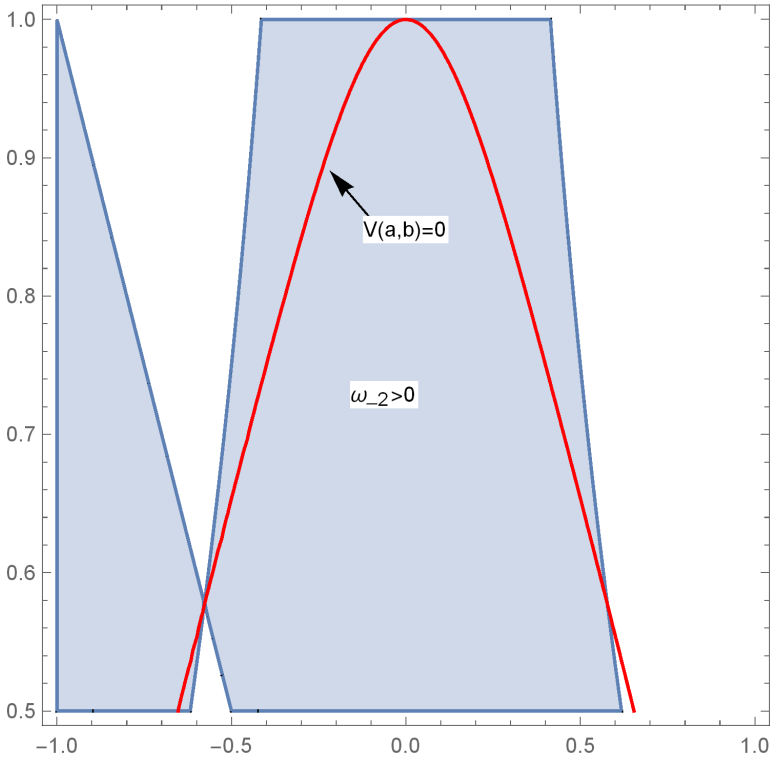

FIGURE 3.2: In the case when $s_{03}=s_{12}$ and $s_{01}=s_{23}$, the intersection of $V(a,b)=0$ and $R_{\omega_0\omega_2}$

mass ratios, we utilize numerical solutions for $V(a,b)=0$ and interpolation to express a as a function dependent on b.

$$b=\phi_1(a)=1-0.022a2.035a^2+0.12a^3+3.62a^4-0.14a^5-3.92a^6 \tag{3.43}$$

This allows us to represent ω_2 as a function of a single variable. Leveraging this approximation, we depict ω_2 in below figure as an estimated function with respect to b. It reveals

that ω_2 decreases as b increases, reaching its maximum value of 1 at $b = 0$, corresponding to the square configuration with four equal masses.

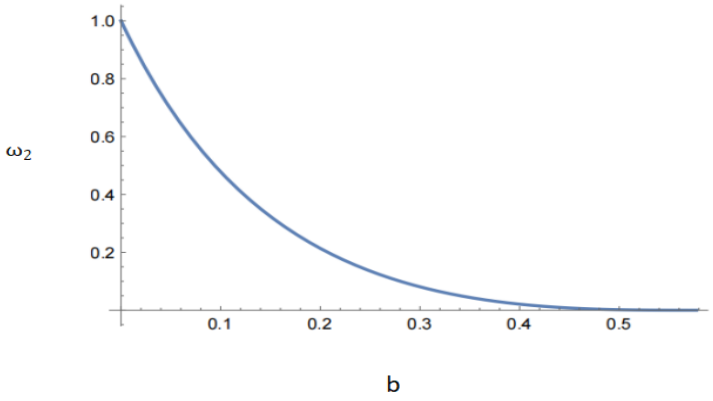

FIGURE 3.3: The approximate values of the mass ratio ω_2 are derived from a relationship with $a = \phi_1(b)$. These values correspond to a set of central configurations, all of which are isosceles trapezoids. When ω_2 equals 1 and b is equal to 0, it results in the square central configuration comprising four equal masses.

Case $s_{03} = s_{12}$ and $s_{01} = s_{02}$; convex and concave kites

Let's examine the scenario where $s_{03} = s_{12}$ and $s_{01} = s_{02}$ which corresponds to $T = \Upsilon$, $\Phi = \Psi$ in the central configuration equations. In this instance, we will refrain from employing theorem (3.11) due to its derivation necessitating $\Phi \neq \Psi$. Instead, by substituting $T = \Upsilon$ and $\Phi = \Psi$ into equations (3.5), we arrive at the condition where $f_{12} = 0$.

$$f_{12} = (d_2 \;\; a\,(d_1 + 1))\,(\frac{1}{X} - \frac{1}{Z}) = 0 \tag{3.44}$$

Consequently, we must possess $d_2 = a(d_1 + 1)$ or $X = Z(s_{13} = s_{23})$. Given that $X = Z$, $T = \Upsilon$, and $\Phi = \Psi$, the equations $f_{01} = 0$, $f_{02} = 0$, *and* $f_{13} = 0$ are utilized to derive the expressions for the mass ratios ω_0, ω_1, and ω_2 as presented below.

$$\begin{aligned}
\omega_0 &= \frac{\Psi^2(Z-\Upsilon)^2(d_2 - ad_1 - a)^2}{Z^2(a-b)(\Upsilon-\Psi)}, \\
\omega_1 &= \frac{\Psi d_1(Z-\Upsilon)}{Z(\Upsilon-\Psi)}, \\
\omega_2 &= \frac{\Psi d_1(Z-\Upsilon)(bd_1 + b - d_2)}{Z(a-b)(\Upsilon-\Psi)}.
\end{aligned} \tag{3.45}$$

The roots are obtained through the concurrent solution of $X = Z$, $T = \Upsilon$, and $\Phi = \Psi$ which are(a, d_1, d_2)

$$(\sqrt{b^2+1}+b,\ -\sqrt{b^2+1}-b, b+1),\ (\sqrt{b^2+1}+b,\ \sqrt{b^2+1}+b,\ b-1). \tag{3.46}$$

Examine the initial solutions given by $a = (\sqrt{b^2+1}+b)$, $d_1 = -a$, and $d_2 = 1+b$. When b is greater than -1, the resulting configurations represent a specific instance of a convex kite with equal diagonals. For situations where b is less than -1, the formations will manifest as concave kites. a square arrangement will be achieved with four masses of equal magnitude when b=0. In the scenario of the unique convex kite, both s_{03} and s_{12} will represent two diagonals of equal length. In the instance of the concave kite, s_{01} and s_{02} will constitute the two adjoining sides of identical length. Demonstrably, the expression $(bd_1 + bd_2)(ab) = d_1$, leading to $\omega_1 = \omega_2$. The mass ratios ω_0 and ω_1 can be expressed as functions of a single variable, as depicted below.

$$\omega_0 = \frac{f_1(b)(1+b^2)^{\frac{5}{2}}(P(b)-\Upsilon(b))^2}{P^2(b)(\Upsilon(b)-\Psi(b))^2},\ \omega_1 = \qquad \frac{(b+\sqrt{1+b^2})\Psi(b)(P(b)-\Upsilon(b)))}{P(b)(\Upsilon(b)-\Psi(b)},$$

where

$$f_1(b) = 2(1+b^2)\sqrt{1+b^2}(1-2b).$$

Given that all components contributing to ω_0 are unequivocally positive functions of b, except for $f_1(b)$, the sign of ω_0 will be determined by $f_1(b)$. The equation $f_1(b) = 0$ can be simplified to a cubic polynomial, specifically $4b^3 + 3_b^2 + 4b + 3 = 0$. The sole real root is located at $b = -\frac{3}{4}$, so at this point $\omega_0 > 0$. The determination of the mass ratio ω_1 hinges on the values of $d_1(b)$, $P(b)\Upsilon(b)$, and $\Upsilon(b)\Psi(b)$. The parameter d_1 is negative for all $b \in \mathbb{R}$, $P\Upsilon$ is negative when $b \in (-\sqrt{3}, \sqrt{3})$, and $\Upsilon - \Psi$ is negative when b is less than $-\frac{1}{\sqrt{3}}$.This indicates that both ω_0 and ω_1 are positive when $b \in (\frac{1}{\sqrt{3}}, \sqrt{3})$. As a result, the parameter $d_2 = b+1 > 0.42$. In such instances, m_3 will consistently lie outside the triangle defined by m_0, m_1, and m_2. Consequently, the resulting configurations will invariably take the form of a convex kite.

In the interval $(0, \sqrt{3})$ for the parameter b, both ω_0 and ω_1 exhibit decreasing trends with respect to b, and $\omega_1(b) > \omega_0(b)$. The maximum values of ω_0 and ω_1 occur at $b = 0$, where $\omega_1(0) = \omega_0(0) = 1$. Refer to figure (5) for the specific values of ω_0 and ω_1.

In the case if another solution arises, where $d_1 = a = b + (b^2 + \sqrt{1})$ and $d_2 = 1 + b$, for positive masses,there are no feasible central configurations. This is because the mass ratio $\omega_0 < 0$ across all values of $b \in \mathbb{R}$.

3.6 Trapezoid Central Configuration for $a \in (0.5, 1)$

To understand the problem better, we will employ the method outlined in above sections to discover central configurations for four instances of the general coplanar 4BP with two pair of same masses. The coordinates for these masses are $m_1(-1, 0)$, $m_2(0, a)$, $m_3(0, b)$ and $m_4(d_1, d_2)$. We fix the $d_1 = -1$, so that all mass ratios remain positive. Now in the case, when $s_{03} = s_{12}$ and $s_{01} = s_{23}$, the intersection of $V(a, b) = 0$ and $R_{\omega_0\omega_2}$ we take the value of $a \in (0.5, 1)$ and find the value of b using the numerical solution.

$$b = \phi_1(a) = 1 - 0.022a2.035a^2 + 0.12a^3 + 3.62a^4 - 0.14a^5 - 3.92a^6. \tag{3.47}$$

Case I: Central Configuration for $a = 0.65$

We choose the $a = 0.65$ and select the $d_1 = -1$ the corresponding value $b = 0.3467538504755$ and $d_2 = 1.15394$. The coordinates for the massses will be $m_1(-1, 0)$, $m_2(0, 0.65)$, $m_3(0, 0.3467538504755)$ and $m_4(-1, 1.15394)$.

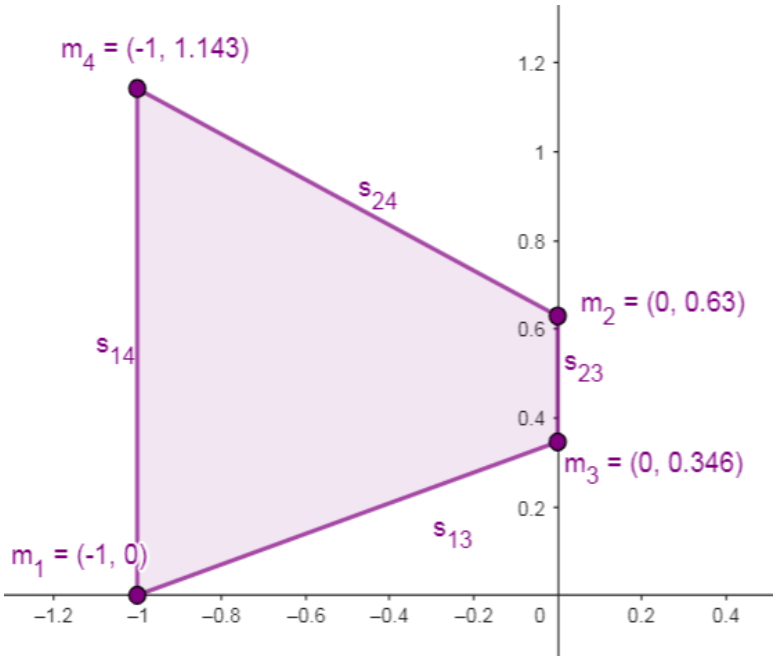

FIGURE 3.4: Central Configuration for $a = 0.65 \in (0.5, 1)$

Case II: Central Configuration for $a = 0.725$

We choose the $a = 0.725$ and select the $d_1 = -1$ the corresponding value $b = 0.400305651$ and $d_2 = 1.12531$. The coordinates for the massses will be $m_1(-1, 0)$, $m_2(0, 0.725)$, $m_3(0, 0.400305651)$ and $m_4(-1, 1.12531)$.

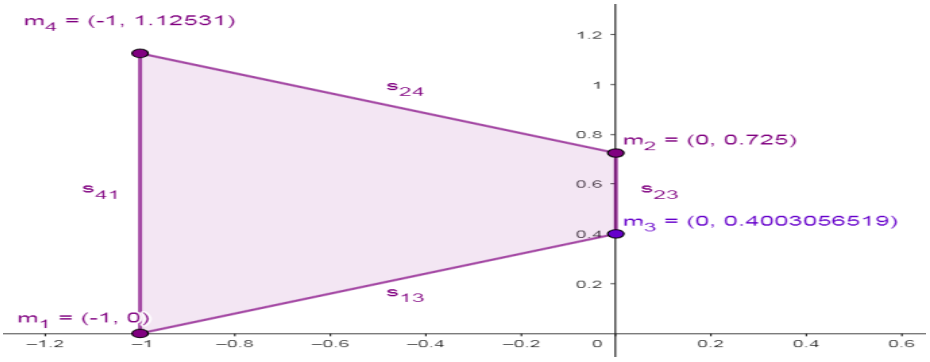

FIGURE 3.5: Central Configuration for $a = 0.725 \in (0.5, 1)$

Case III: Central Configuration for $a = 0.80$

We choose the $a = 0.80$ and select the $d_1 = -1$ the corresponding value $b = 0.3467538$ and $d_2 = 1.14675$. The coordinates for the massses will be $m_1(-1, 0)$, $m_2(0, 0.80)$, $m_3(0, 0.3467538)$ and $m_4(-1, 1.14675)$.

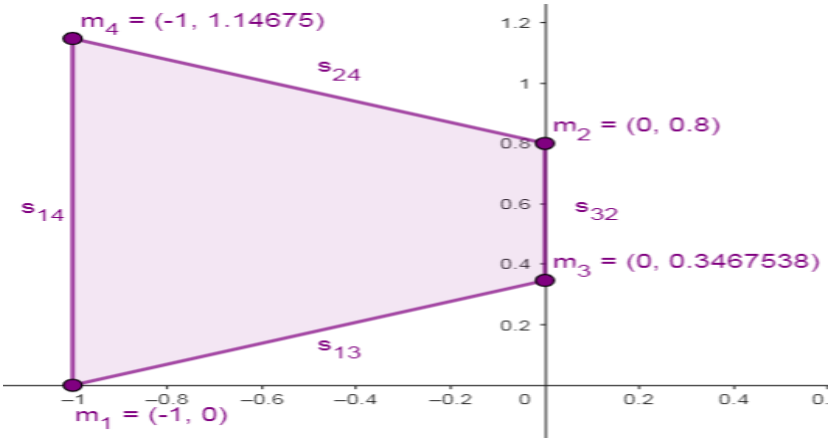

FIGURE 3.6: Central Configuration for $a = 0.8 \in (0.5, 1)$

Case IV: Central Configuration for $a = 0.95$

We choose the $a = 0.95$ and select the $d_1 = -1$ the corresponding value $b = 0.157594$ and $d_2 = 0.13$. The coordinates for the massses will be $m_1(-1, 0)$, $m_2(0, 0.95)$, $m_3(0, 0.157594)$ and $m_4(-1, 0.13)$.

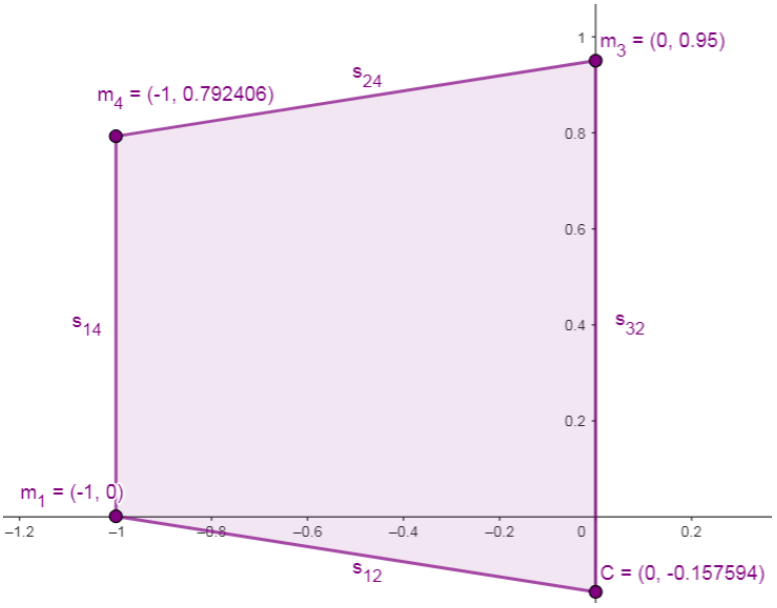

FIGURE 3.7: Central Configuration for $a = 0.95 \in (0.5, 1)$

In next chapter, the equilibrium points for these four cases, their stability and Newton Basin of Attraction for them will be discussed.

Chapter 4

Dynamic of the Fifth Body in Restricted Isoceles Trapezoid

In this extension work, a restricted scenario featuring four bodies is explored, with four distinct positive masses denoted as m_1, m_2, m_3, m_4 arranged in a fixed isosceles trapezoid. This scenario is referred to as 'The Restricted Trapezoidal Five-Body Problem'. Three of these masses are situated at the corners of a triangle, while the fourth mass has the flexibility to inhabit any point within the plane, thereby forming either convex or concave central configurations. Meanwhile, a smaller mass identified as m_5 traverses the identical plane, under the influence of gravitational forces exerted by the four main masses ($m_1,\ m_2,\ m_3,\ m_4$). It is essential to highlight that the motion of m_5 does not impact the displacement of the four primary masses. So first we have to find the equation of motion and find the equilibrium points for the fifth body and secondly find Newton's Basin of attraction for equilibrium points. To analyze the fifth body in the isosceles trapezoid problem, the main objective is to find the equilibrium points for the restricted body, determine the Newton Basin of Attraction for these equilibrium points, and subsequently assess the stability of these points. The objective of this study to investigate the behavior of system near these equilibrium points.

This section studies the motion of a fifth particle m_4 in a plane, influenced by the gravity of four other particles arranged in a fixed isosceles trapezoid (as shown previously). Now we set a restricted isosceles trapezoid five-body problem. We are considering two positive masses m_1 and m_3 to be equal. By fixing $d_1 = -1$, m_2 becomes equal to m_4. Two

pairs of identical masses are positioned at adjacent vertices, maintaining motion that consistently forms an isosceles trapezoid configuration. It's assumed that a very small mass, denoted as m_5, moves within the same plane as the larger masses and does not affect the motion of the primary four. Firstly, examine the motion of the small mass m_5 within this plane influenced solely by the gravitational forces of the four primaries and analyze the trajectory of mass m_5 and employ contour plots to identify potential equilibrium solutions. And then conclude by determining Newton's basins of attraction concerning these equilibrium points. Considering the inertial frame of reference and Newton law of gravitation, the equation of motion for the four positive bodies is as follow:

$$m_i \ddot{s_i} = \bigtriangledown_i J_i \; i = 1, 2, 3, ..., n,$$

$$\ddot{s_i} = -G \sum_{j=1, i \neq j}^{n} m_j \frac{\mathbf{s}_j - \mathbf{s}_i}{|\mathbf{s}_j - \mathbf{s}_i|}, \tag{4.1}$$

where G is the Gravitational constant and m_i and s_i are mass and position vector of i^{th} body. The masses lie in the same plane but are not in a straight line. The position vector of our 4BP are; $s_1 = (-1, 0)$, $s_2 = (0, a)$, $s_3 = (0, b)$ and $s_4 = (d_1, d_2)$ where a, b, d_1 and d_2 are real. So the movement of the infinitesimally small body denoted as m_5, influenced by the gravitational pull of the five primary bodies. It is assumed that the mass of the fifth body is notably smaller than the masses of the primary bodies ($m_5 \ll m_1,\ m_2, m_3,\ m_4$). Consequently, the fifth body functions as an infinitesimal test particle, and as such, it has negligible impact on the motion of the four primary bodies. The equation of motion of m_5 in the gravitational field of m_1 to m_4 is:

$$\ddot{s_5} = m_1 \frac{\mathbf{s}_5 - \mathbf{s}_1}{|\mathbf{s}_5 - \mathbf{s}_1|^3} + m_1 \frac{\mathbf{s}_5 - \mathbf{s}_2}{|\mathbf{s}_5 - \mathbf{s}_2|^3} + m_2 \frac{\mathbf{s}_5 - \mathbf{s}_3}{|\mathbf{s}_5 - \mathbf{s}_3|^3} + m_3 \frac{\mathbf{s}_5 - \mathbf{s}_4}{|\mathbf{s}_5 - \mathbf{s}_4|^3}. \tag{4.2}$$

We are about to define a coordinate system that uniformly rotates a round the center of mass, identified as ω. Within this newly rotating frame, consider (x, y) are the coordinates of m_5.

The goal is to convert the equation from its original fixed inertial frame to this rotating coordinate system, employing the provided orthogonal system.

$$\mathbf{e_1} = e^{i\omega t}, \quad \mathbf{e_2} = ie^{i\omega t},$$

In the context ω denotes the angular speed and t represents time, the position vector of m_5 can be expressed as follows:

$$\mathbf{s_5} = x(t)\mathbf{e_1} + y(t)\mathbf{e_2}. \tag{4.3}$$

Selecting ω without any loss of generality and computing the first and second derivatives of equation (4.3) results in:

$$\dot{\mathbf{s_5}} = [(\dot{x} - y) + i(x + \dot{y})]e^{it},$$

$$\ddot{\mathbf{s_5}} = [(\ddot{x} - 2\dot{y} - x) + i(\ddot{y} + 2\dot{x} - y)]e^{it}. \tag{4.4}$$

Upon substituting equation (4.4) into equation (4.2), we can formulate in the rotating frame the equations describing the motion of m_5 in component form as follows:.

$$\ddot{x} - 2\dot{y} = x - \left[m_0\frac{x}{s_{51}^3} + m_1\frac{x+1}{s_{52}^3} + m_2\frac{x}{s_{53}^3} + m_3\frac{x-d_1}{s_{54}^3}\right], \tag{4.5}$$

$$\ddot{y} + 2\dot{x} = y - \left[m_0\frac{y-b}{s_{51}^3} + m_1\frac{y}{s_{52}^3} + m_2\frac{y-a}{s_{53}^3} + m_3\frac{y-d_2}{s_{54}^3}\right], \tag{4.6}$$

where the mutual distances are defined as follows:

$$s_{51} = \sqrt{x^2 + (y-b)^2},$$

$$s_{52} = \sqrt{(x+1)^2 + y^2},$$

$$s_{53} = \sqrt{x^2 + (y-a)^2},$$

$$s_{54} = \sqrt{(x-d_1)^2 + (y-d_2)^2}.$$

The alternative expression for the m_5 equation of motion in the plane of primaries is as follows:

$$U_x = \frac{\partial U}{\partial x} = \ddot{x} - 2\dot{y}, \tag{4.7}$$

$$U_y = \frac{\partial U}{\partial y} = \ddot{y} + 2\dot{x}, \tag{4.8}$$

where the effective potential $U(x, y)$ is:

$$U(x,y) = \frac{x^2+y^2}{2} + \left[\frac{m_1}{\sqrt{x^2+(y-b)^2}} + \frac{m_2}{\sqrt{(x+1)^2+y^2}} + \frac{m_3}{\sqrt{x^2+(y-a)^2}} + \frac{m_4}{\sqrt{(x-d_1)^2+(y-d_2)^2}} \right]. \quad (4.9)$$

By comparing equations (4.5)-(4.8), the equation of motion for the secondary body can be formulated as,

$$U_x(x,y) = x - \left[m_1 \frac{x}{s_{51}^3} + m_2 \frac{x+1}{s_{52}^3} + m_3 \frac{x}{s_{53}^3} + m_4 \frac{x-d_1}{s_{54}^3} \right],$$
$$U_y(x,y) = y - \left[m_1 \frac{y-b}{s_{51}^3} + m_2 \frac{y}{s_{52}^3} + m_3 \frac{y-a}{s_{53}^3} + m_4 \frac{y-d_2}{s_{54}^3} \right].$$

We can utilize both equations to ascertain the positions of the equilibrium points. These points correspond to locations in space where the infinitesimal mass m_4 exhibits zero velocity and acceleration, effectively remaining at rest in relation to the primaries m_1, m_2, m_3, and m_4 respectively. When situated at an equilibrium point (commonly referred to as a libration point or Lagrange point), an object will seemingly remain stationary. These solutions are derivable only when meeting the necessary condition of all rates equating to zero. The hill region is another name for the authorized motion area. The Jacobian constant is defined as follows:

$$C + U = \frac{1}{2}(\dot{x}^2 + \dot{y}^2) = v^2. \quad (4.10)$$

For a given Jacobi constant value, the square of velocity (v^2) is entirely determined by the position in the rotating frame.

Since v^2 cannot assume negative values, this implies that...

$$C + U \geq 0. \quad (4.11)$$

The boundaries distinguishing regions where motion is permissible from those where it is not are determined by setting v^2 equal to zero.

$$C + U = 0. \quad (4.12)$$

4.1 Contour Plot for $a \in (0.5, 1)$

4.1.1 Case I: $a = 0.65$

When $a \in (0.5, 1)$, we choose $a = 0.65$ to be a point in the interval, the corresponding value of $b = 0.3467538504755, d_1 = -1$ and $d_2 = 1.15394$. The value of mass $m_1 = m_3 = 1$ and $m_2 = m_4 = 0.00151377$ almost negligible with respect to masses m_1 and $m_3 = 1$. The zero velocity curve, hill spheres depicted in figure 4.1, are circular areas surrounding the primary masses. Equation (4.13) suggests that $C+U$ needs to be greater

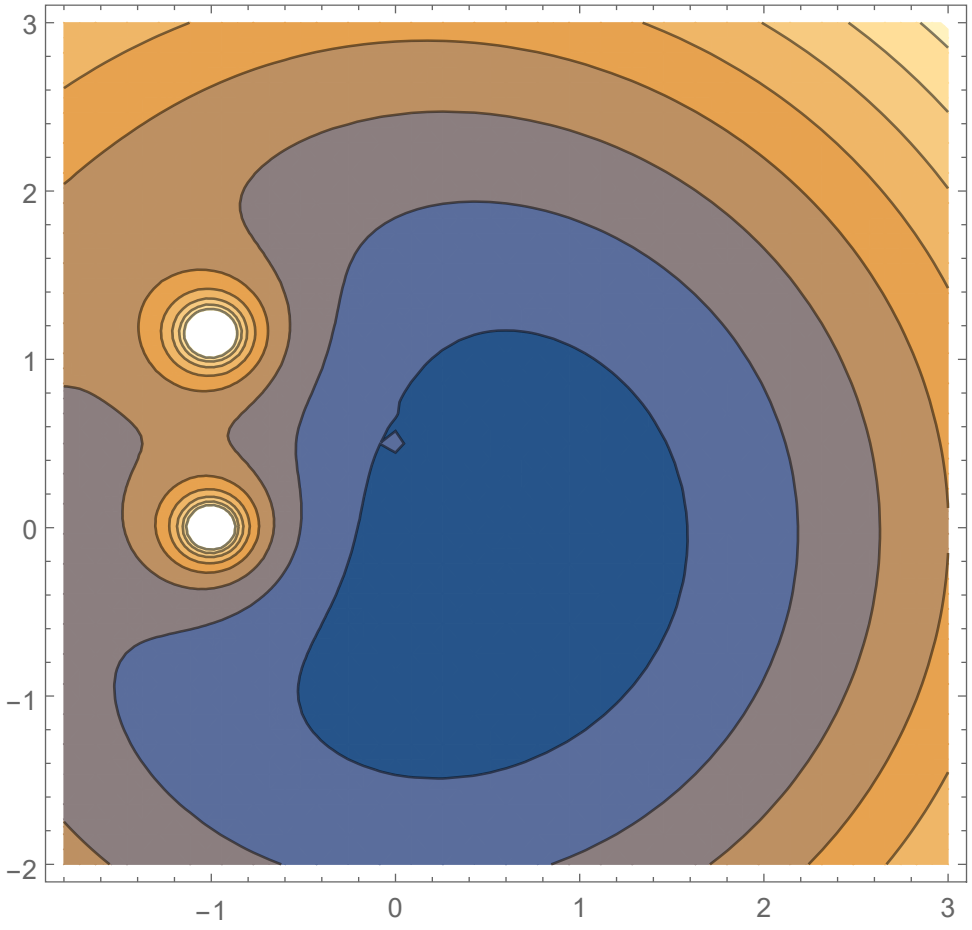

FIGURE 4.1: Case I: Zero velocity curve for mass ratios $\omega_0 = 0.00151377$, $\omega_1 = 1$, $\omega_2 = 0.00151377$.

than or equal to 0. This implies that by setting U equal to C, a boundary can be established to differentiate between allowed and forbidden regions for motions. In this case the feasible region of motion for the infinitesimal mass m_5 is illustrated in Figure (4.2) for various values of the Jacobin constant (C), where $\omega_1 = 0.00151377$, $\omega_2 = 1$

and $\omega_3 = 0.00151377$. Different values of C show the different energy level showed by different color. Shaded areas represent the permitted motion regions for m_5. Numerical analysis confirmed that these permitted regions are interconnected when C is less than or equal to 4. As C increases, the interconnected permitted regions gradually disconnect, culminating in complete disconnection at $C = 6$. Noteworthy is the observation that the disconnection occurs in five stages, ultimately confining m_5 entirely within the shaded region when C is greater than or equal to 4.

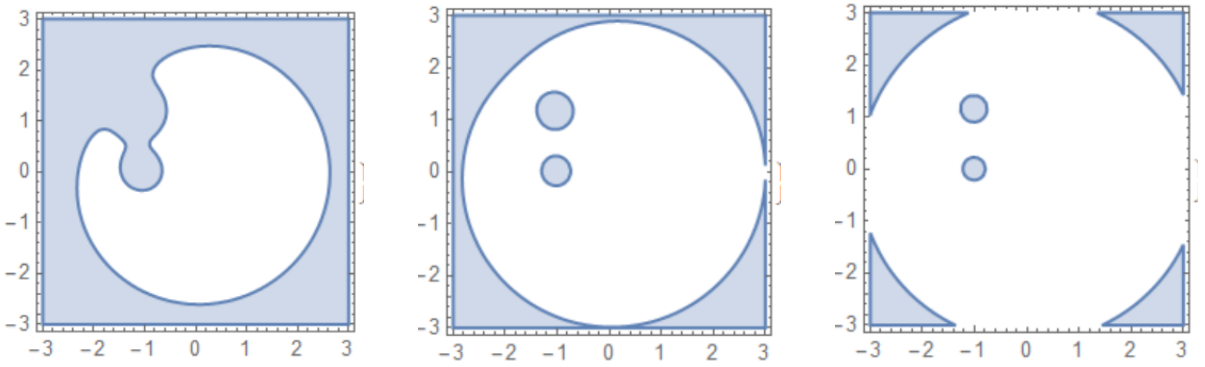

(a) (b) (c)

FIGURE 4.2: Case I: Areas of motion for the infinitesimal mass m_5. (a) $C = 4$ (b) $C = 5$ (c) $C = 6$

Contour Plot for Motion for Restricted body in Case I

We show the contour plot for equations of motion for restricted body. Blue line show that $f_1 = 0$ at that points and Orange line show that $f_2 = 0$ at that points. Black dots show the position of primaries m_i where $i = (1, 2, 3, 4)$ and red dots represents the position of Lagrange points. Contour plot for these values show that, it has five Lagrange points:

$L_1 = (-0.02938761600539582, 0.6624051471197344)$,

$L_2 = (-0.02900849278442055, 0.5170578895199723)$,

$L_3 = (-1.5257394204223007, 1.6424128926413448)$,

$L_4 = (-1.1108069559787692, 0.5477592785128903)$

$L_5 = (0.5716802613355917, -0.20575927206030944)$.

Contour plot for these values show that the L_1, L_2 are collinear.

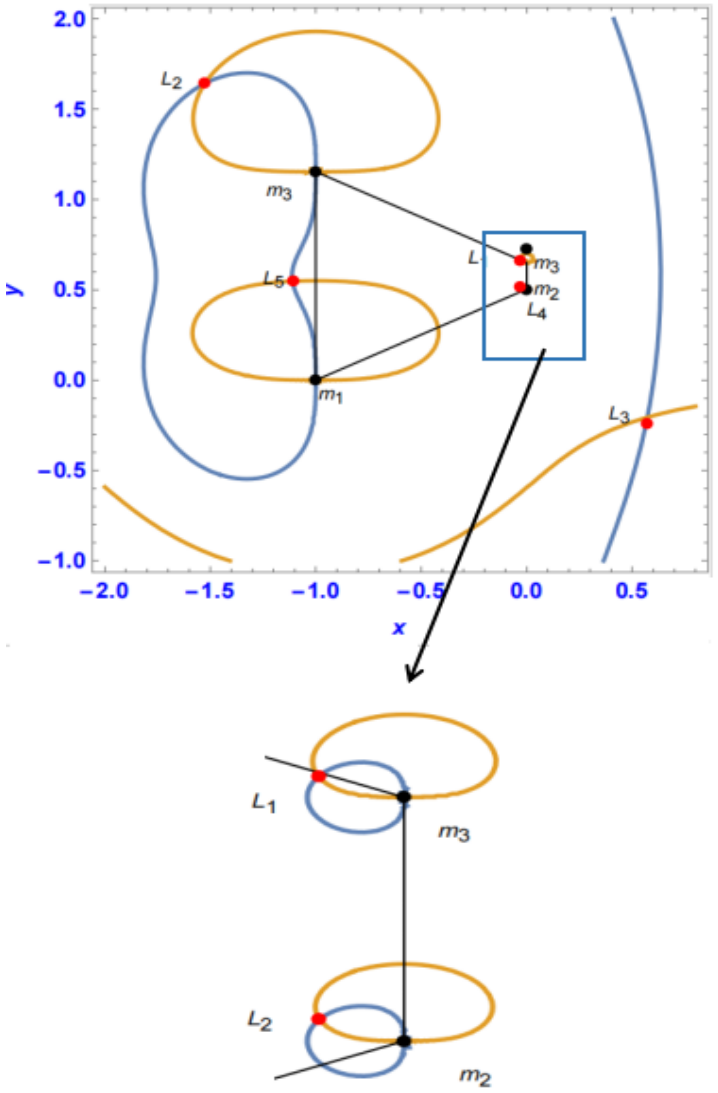

FIGURE 4.3: Contour plot for $a = 0.65$. $f_1 = 0$ (blue) and $f_2 = 0$ (orange) Black dots show the position of primary masses and red dots represents the position of Lagrange points.

4.1.1.1 Basin of Attraction for Case I

We start our analysis with this case, the Newton-Raphson of attraction in the xy-configuration plane, where five equilibrium points are present. Here $a = 0.65$ and $b = 0.3467538504755$.

The different color indicate the convergence to a specific equi-librium points. The equilibrium points are marked using following colors

L_1(Brown), L_2(Red), L_3(Blue), L_4(Magenta), L_5(Green) and white show the non converging area.

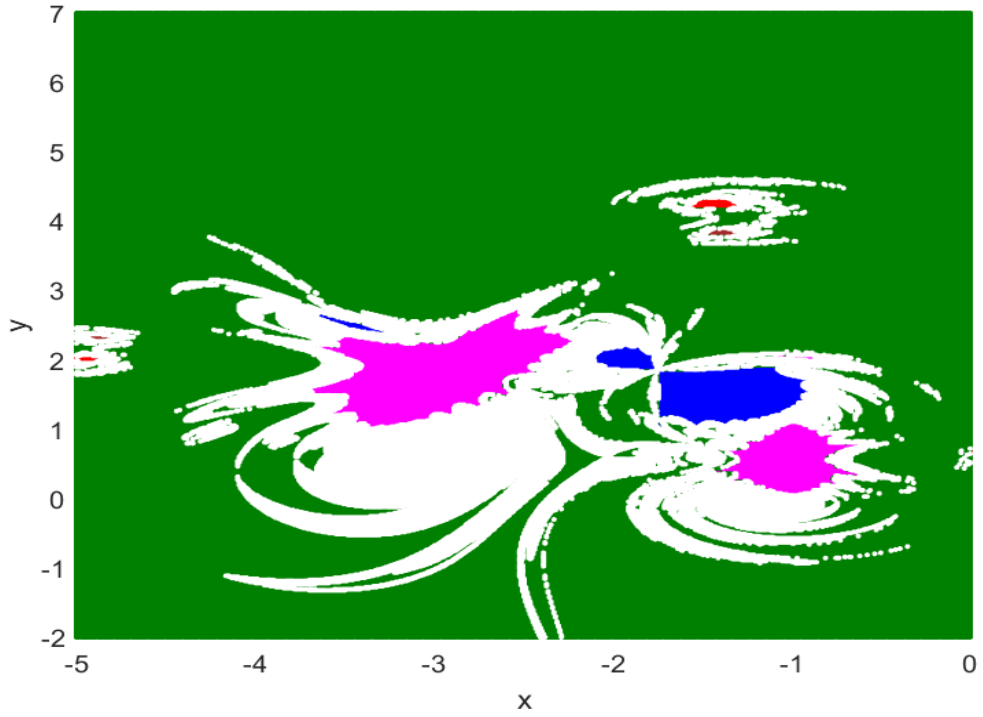

FIGURE 4.4: The Newton-Raphson of attraction in the xy-configuration plane, where five equilibrium points are present. Here $a = 0.65$ and $b = 0.34675385047552$. Initial conditions leading to specific equilibrium points are marked with distinct colors L_1 (Brown), L_2 (Red), L_3 (Blue), L_4 (Magenta), L_5 (Green) and white show the non converging area.

4.1.2 Case II: $a = 0.725$

We choose $a = 0.725$ to be a point in the interval $a \in (0.5, 1)$, the corresponding value of $b = 0.40030565190950845$, $d_1 = -1$ and $d_2 = 1.12531$. The value of $m_1 = m_3 = 1$ and $m_2 = m_4 = 0.0206726$ almost negligible with respect to $m_1 = m_3$.

The zero velocity curve, hill spheres, depicted in below figure, are circular areas surrounding the primary masses. In case II the feasible motion region for the infinitesimal mass m_5 is illustrated in figure (4.2) for various values of the Jacobian constant (C), where $\omega_1 = 0.00151377$, $\omega_2 = 1$ and $\omega_3 = 0.00151377$. Shaded areas represent the permitted motion regions for m_5. Through numerical analysis, it is confirmed that these permitted regions are

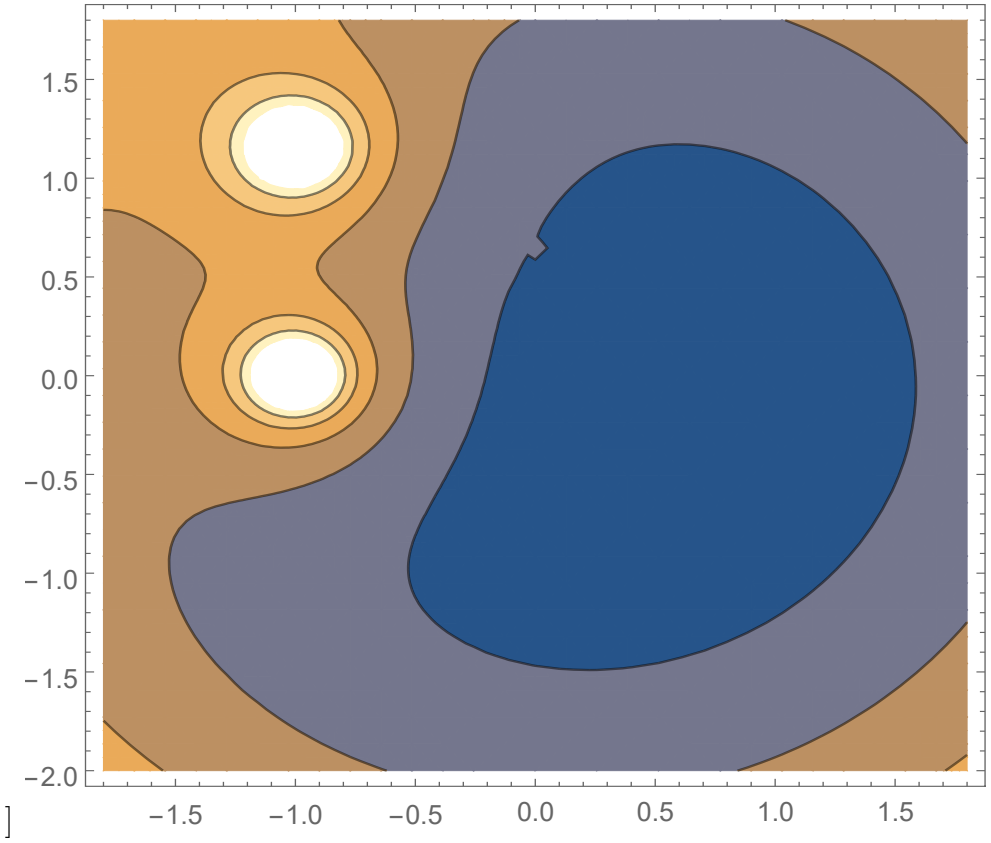

FIGURE 4.5: Zero Velocity Curve for $a = 0.725$ where all mass ratios $\omega_0 = 0.00151377$, $\omega_1 = 1$, and $\omega_2 = 0.00151377$ are positive

interconnected when C is less than or equal to 6. As C increases, the interconnected permitted regions gradually disconnect, culminating in complete disconnection at C= 6. Noteworthy is the observation that the disconnection occurs ultimately confining m_5 entirely within the shaded region when C is greater than or equal to 6.

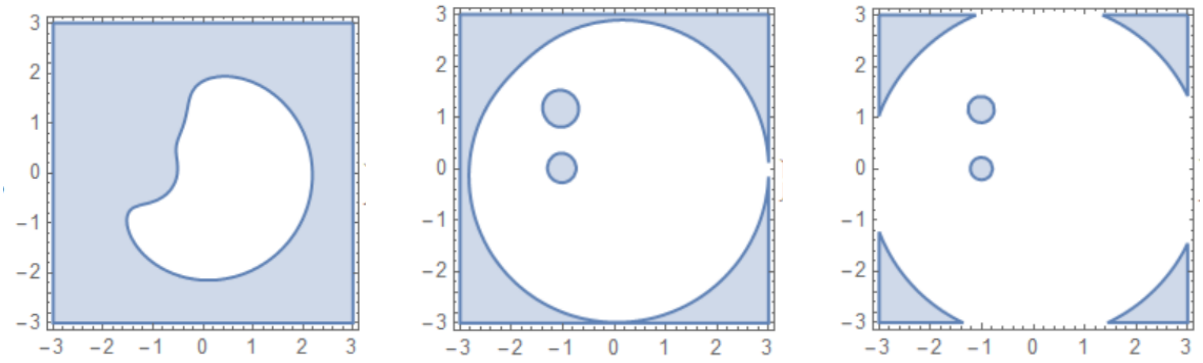

(a) (b) (c)

FIGURE 4.6: Case I: Areas of motion for the infinitesimal mass m_5. (a) $C = 4$ (b) $C = 5$ (c) $C = 6$

Contour Plot for Equations of Motion for Restricted body

We show the contour plot for equations of motion for restricted body. Orange line show that $f_2 = 0$ at that points and blue line show that $f_1 = 0$ at that points. Contour plot for these values show that, it has five Lagrange points

$L_1 = (-1.539069319851305, 1.609026264128955)$,

$L_2 = (-0.10427278743073057, 0.7609952888468957)$,

$L_3 = (-0.10063382638239718, 0.44617857089680274)$,

$L_4 = (-1.0979955863457733, 0.5365706938164287)$,

$L_{=}5(0.5844395174347283, -0.2420797788046294)$.

Contour plot for these values show that the L_1, L_4 are colinear.

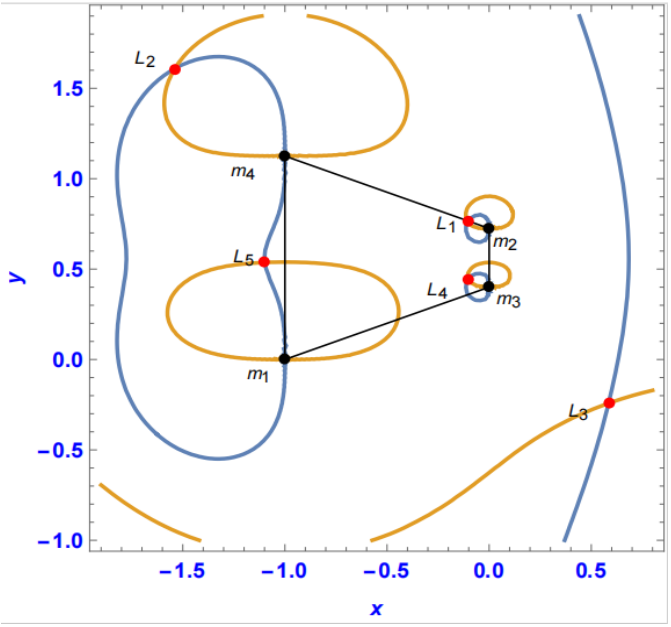

FIGURE 4.7: Contour plot for $a = 0.725$. Black dots show the position of primaries m_i where $i = (0, 1, 2, 3)$ and red dots represents the position of Lagrange points. $f_1 = 0$ (blue) and $f_2 = 0$ (orange).

4.1.2.1 Basin of Attraction for Case II

In this case, the Newton-Raphson of attraction in the xy-configuration plane, where five equilibrium points are present. Here $a = 0.725$ and $b = 0.40030565190950845$. Each distinct colored region represents convergence to a specific equilibrium point. The equilibrium points are marked using following colors L_1(Brown), L_2(Red), L_3(Blue), L_4(Magenta), L_5(Green) and white show the non converging area.

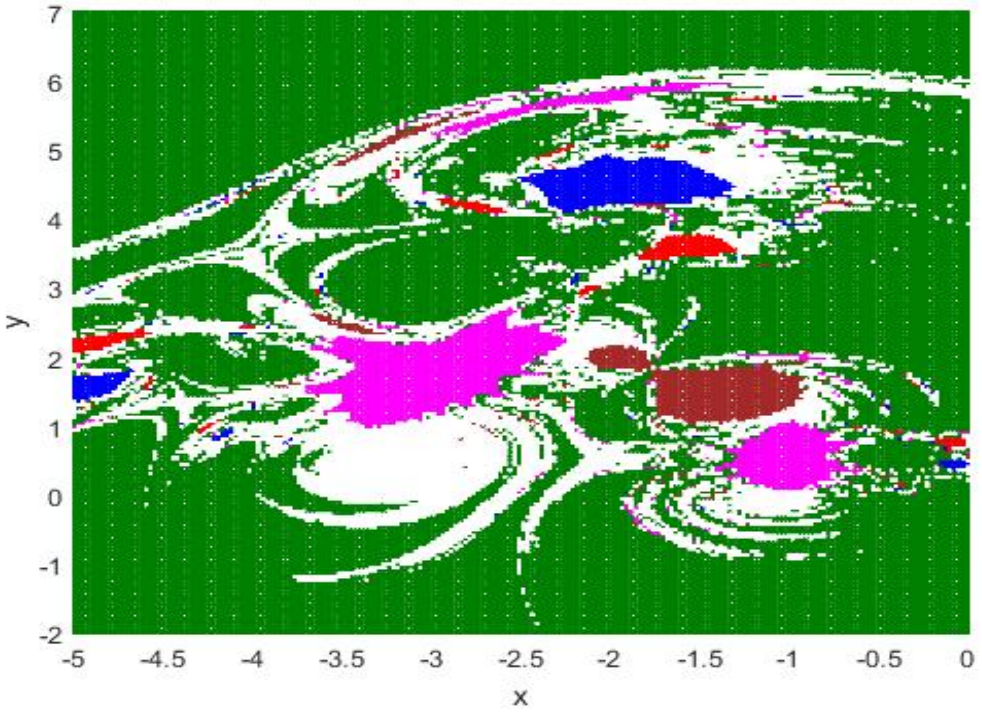

FIGURE 4.8: The Newton-Raphson of attraction in the xy- configuration plane, where five equilibrium points are present. Here $a = 0.725$ and $b = 0.34675385047552$. Initial conditions leading to specific equilibrium points are marked with distinct colors L_1(Brown), L_2(Red), L_3(Blue), L_4(Magenta), L_5(Green) and white show the non converging area.

4.1.3 Case III: $a = 0.8$

When $a \in (0.5, 1)$, we take $a = 0.8$ to be any point in the interval, the corresponding value of $b = 0.3467538504755$, $d_1 = -1$ and $d_2 = 1.14675$. The value of mass $m_1 = m_3 = 1$ and $m_2 = m_4 = 0.0460913$ almost negligible with respect to masses m_1 and $m_3 = 1$. The zero velocity curve (hill spheres), depicted in figure below are circular areas surrounding the primary masses.

In case III the feasible motion region for the infinitesimal mass m_5 is illustrated in figure (4.2) for various values of the Jacobian constant (C), where $\omega_1 = 0.00151377$, $\omega_2 = 1$ and $\omega_3 = 0.00151377$. Shaded areas represent the permitted motion regions for m_5. Through numerical analysis, it is confirmed that these permitted regions are interconnected when C is less than or equal to 8.

As C increases, the interconnected permitted regions gradually disconnect, culminating

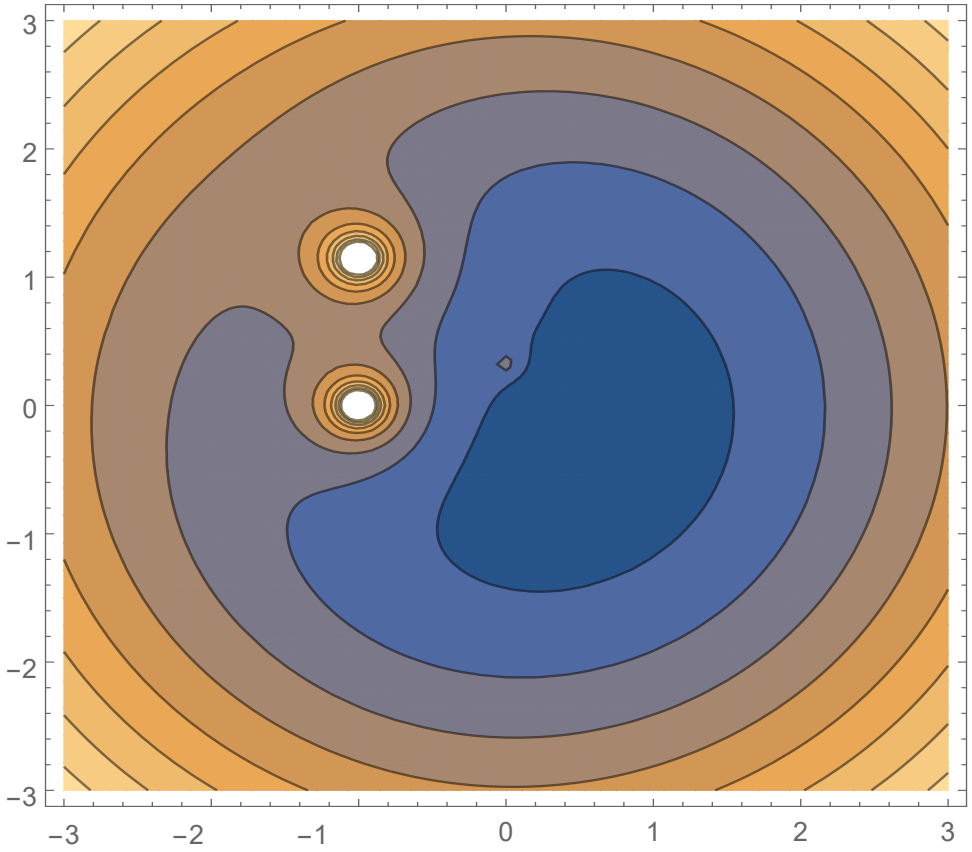

FIGURE 4.9: Zero Velocity Curve for $a = 0.8$ where all mass ratios $\omega_0 = 0.0460913$, $\omega_1 = 1$ and $\omega_2 = 0.0460913$ are positive

in complete disconnection at $C = 8$.

Noteworthy is the observation that the disconnection occurs ultimately confining m_5 entirely within the shaded region when C is greater than or equal to 8.

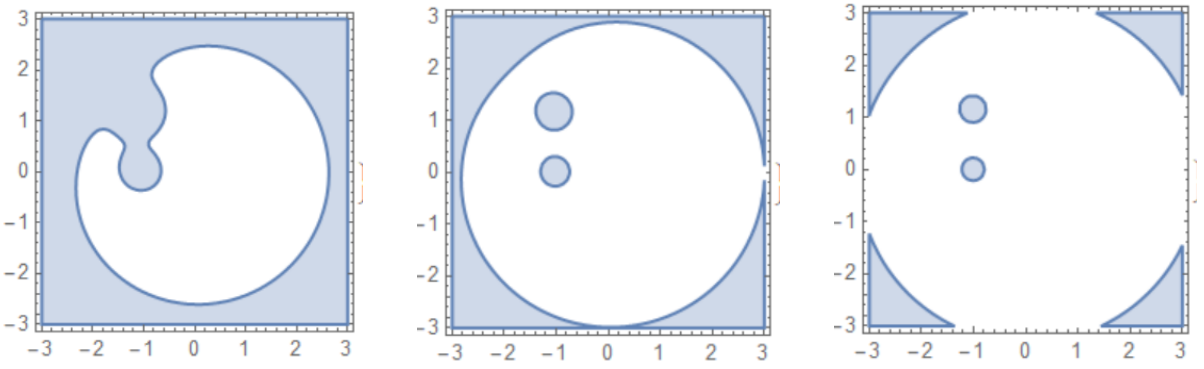

(a) (b) (c)

FIGURE 4.10: Case I: Areas of motion for the infinitesimal mass m_5. (a) $C = 4$ (b) $C = 5$ (c) $C = 6$

We show the contour plot for equations of motion for restricted body.Orange line show that $f_2 = 0$ at that points and blue line show that $f_1 = 0$ at that points. Contour plot for these values show that, it has five Lagrange points:

$L_1 = (-1.5297129163825713, 1.63825487066042)$,

$L_2 = (-0.14889281745533264, 0.8516062353651818)$,

$L_3 = (-0.14811155872721168, 0.40778626770681287)$,

$L_4 = (0.5943717266335518, -0.2834474820752444)$,

$L_5 = (-1.1000476120727627, 0.5452856496893987)$.

Contour plot for these values show that the L_1, L_4 are collinear.

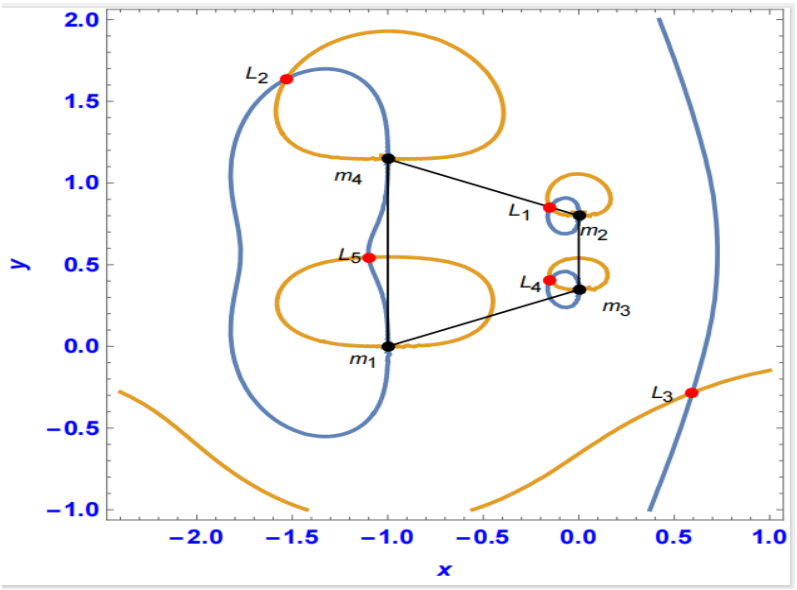

FIGURE 4.11: Contour plot for $a = 0.8$. Black dots show the position of primaries m_i where $i = (0, 1, 2, 3)$ and red dots represents the position of Lagrange points. $f_1 = 0$(blue) and $f_2 = 0$ (orange).

4.1.3.1 Basin of Attraction Case III

In this case, where five equilibrium points are present.

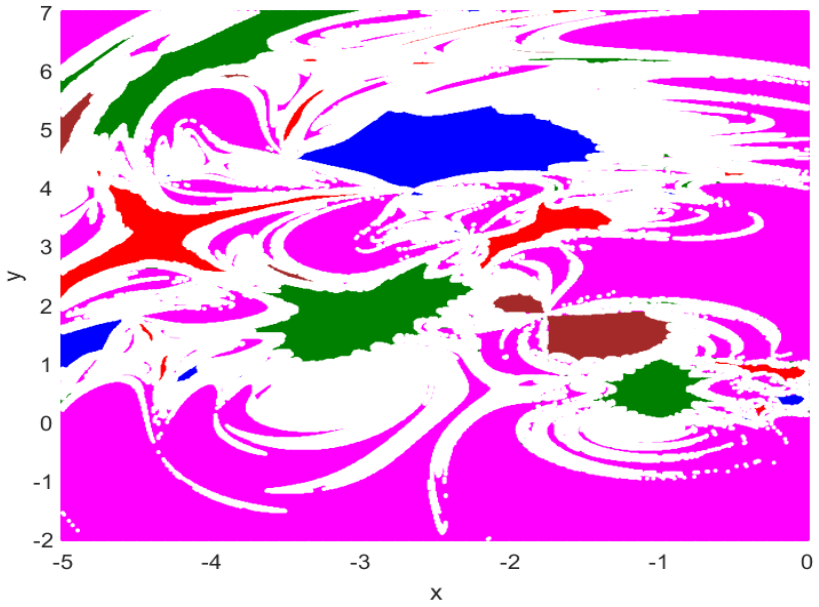

FIGURE 4.12: The Newton-Raphson of attraction in the xy-configuration plane, where five equilibrium points are p resent. Here $a = 0.8$ and b =0.34675385047552. Initial conditions leading to specific equilibrium points are marked with distinct colors L_1(Brown), L_2(Red), L_3(Blue), L_4(Magenta), L_5('Dark Red') and white show the non converging area.

4.1.4 Case IV: $a = 0.95$

When $a \in (0.5, 1)$, we take $a = 0.95$ to be any point in the interval, the corresponding value of $b = -0.157594$, $d_1 = -1$ and $d_2 = 0.792406$. The value of mass $m_1 = m_3 = 1$ and $m_2 = m_4 = 3.28342$. The zero velocity curve, hill spheres, depicted in below figure, are circular areas surrounding the primary masses.

In this case I the feasible motion region for the infinitesimal mass m_5 is illustrated in figure (4.2) for various values of the Jacobian constant (C), where $\omega_1 = 0.00151377$, $\omega_2 = 1$ and $\omega_3 = 0.00151377$. Shaded areas represent the permitted motion regions for m_5.

Through numerical analysis, it is confirmed that these permitted regions are interconnected. As C increases, the intercon-nected permitted regions gradually disconnect, culminating in complete disconnection at C= 12. Noteworthy is the observation that the disconnection occurs in five stages, ulti-mately confining m_5 entirely within the shaded region when C is greater than or equal to 12.

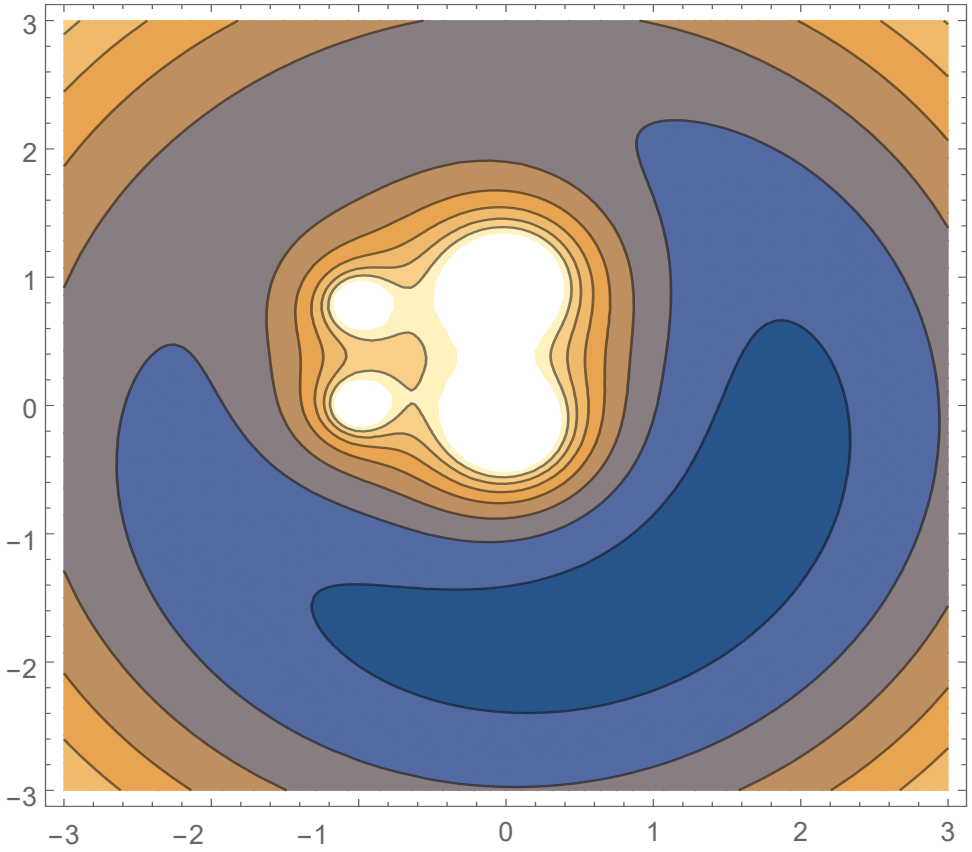

FIGURE 4.13: Zero Velocity Curve for $a = 0.95$ where all mass ratios $\omega_0 = 3.28342$, $\omega_1 = 1$, $\omega_2 = 3.28342$ are positive

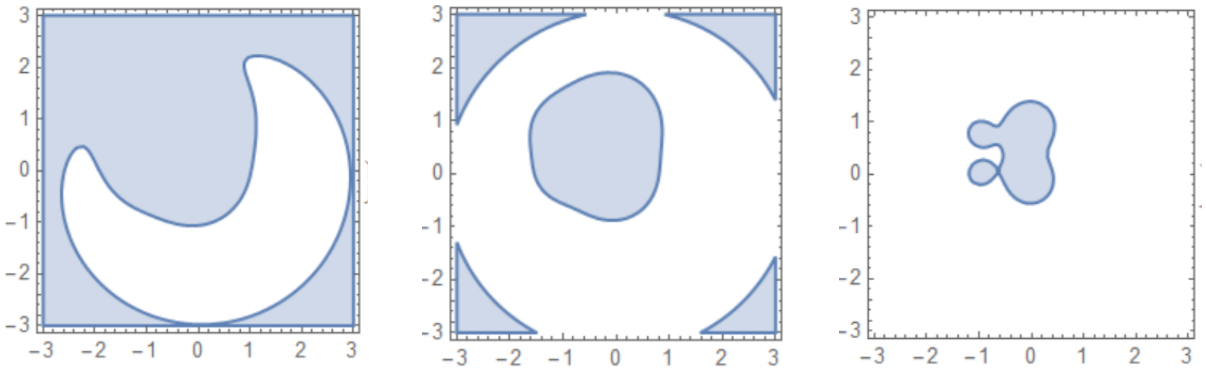

(a) (b) (c)

FIGURE 4.14: Case I: Areas of motion for the infinitesimal mass m_5. (a) $C = 7$ (b) $C = 8$ (c) $C = 12$

We show the contour plot for equations of motion for restricted body. Orange line show that $f_12 = 0$ at that points and blue line show that $f_1 = 0$ at that points.

Contour plot for these values show that, it has five Lagrange points

$L_1 = (-0.9155242710659137, 2.2297429430870928)$,

$L_2 = (1.2282884672972298, -1.3534240360776302)$,

$L_3 = (-0.6352345812853883, 0.7654426569688555)$,

$L_4 = (-0.04646587652521089, 0.3909700807909814)$,

$L_5 = (-0.6346636374668658, 0.06441693377203969)$.

Contour plot for these values show that the L_3, L_5 are collinear.

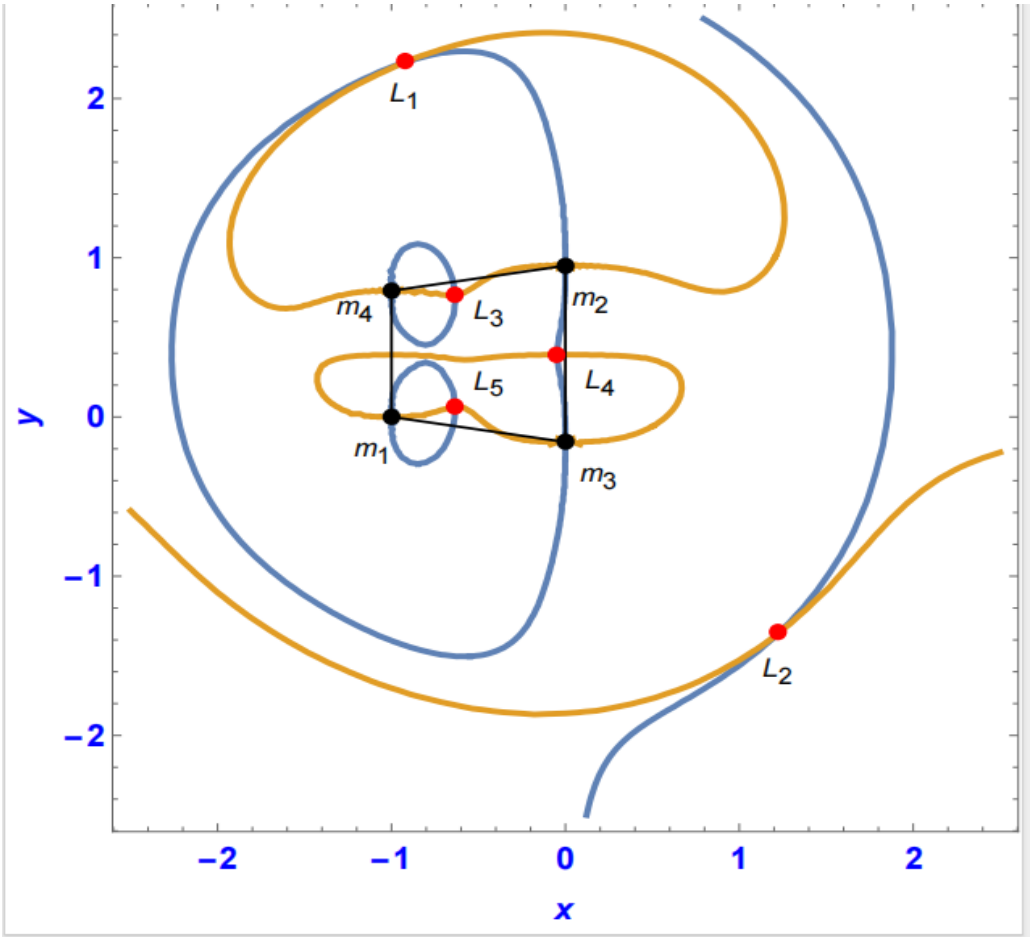

FIGURE 4.15: Contour plot for $a = 0.95$

4.1.4.1 Basin of Attraction Case IV

In this case,the Newton-Raphson of attraction in the xy-configuration plane, where five equilibrium points are present. Here $a = 0.95$ and $b = -0.15759414444696293$. Each distinct color or region represents convergence to a specific equilibrium point. The different convergence areas are marked using following colors L_1(Brown), L_2(Red), L_3(Blue), L_4(Magenta), L_5(Green) and white show the non converging area.

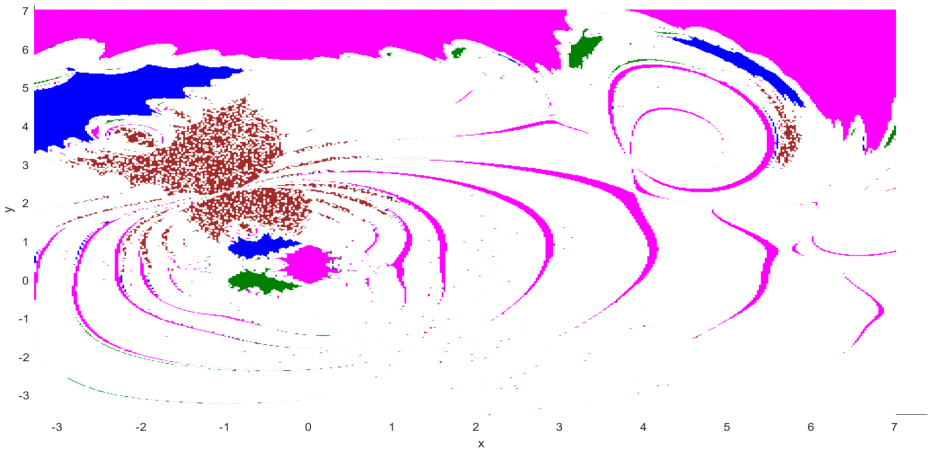

FIGURE 4.16: The Newton-Raphson of attraction in the xy-configuration plane, where five equilibrium points are present. Here $a = 0.95$ and $b = -0.15759414444696293$. Initial conditions leading to specific equilibrium points are marked with distinct colors L_1(Brown), L_2(Red), L_3(Blue), L_4(Magenta), L_5(Green) and white show the non converging area.

4.2 Stability Analysis of Equilibrium Points

To assess the stability of the equilibrium points identified earlier, we will utilize the conventional approach of linearization. This involves linearizing the equation of motion for a small mass.

Let's denote the coordinates of an equilibrium point in the Restricted Five-Body Problem (RR5BP) as (x, y). Suppose there's a slight displacement (X, Y) from this point, resulting in the new positions $x + X$ and $y + Y$ for the secondary mass.

By employing Taylor's series expansion on equations (4.7) and (4.8), we obtain a fresh set of second-order linear differential equations. [39].

$$\left.\begin{aligned} \ddot{X} - 2\dot{Y} &= XU_{xx} + YU_{xy}, \\ \ddot{Y} + 2\dot{X} &= XU_{xy} + YU_{yy}. \end{aligned}\right\} \tag{4.13}$$

The matrix representation of the linearized equations 4.13 is shown as follows:

$$\dot{\mathbf{X}} = \mathbf{AX},$$

$$\dot{\mathbf{X}} = \begin{pmatrix} \dot{x} \\ \dot{y} \\ \ddot{x} \\ \ddot{y} \end{pmatrix}, \mathbf{A} = \begin{bmatrix} 0 & 0 & 1 & 0 \\ 0 & 0 & 0 & 1 \\ U_{xx} & U_{xy} & 0 & 2 \\ U_{xy} & U_{yy} & -2 & 0 \\ . & & & \end{bmatrix} \tag{4.14}$$

The characteristic equation for the given matrix A is:

$$p(\lambda) = \lambda^4 - (U_{xx} + U_{yy})\lambda^2 + (U_{xx}U_{yy} - U_{xy}^2 - 4) = 0$$

We put $\alpha = U_{xx} + U_{yy}$ and $\beta = U_{xx}U_{yy} - U_{xy}^2 - 4$. Let $\lambda_2 = \lambda$, then the characteristic equation for the given matrix A becomes:

$$p(\lambda) = \lambda^2 - \alpha\lambda + \beta = 0$$

For a Lagrange point to exhibit linear stability against minor disturbances, it necessitates that all four roots, denoted as λ in above equation, are purely imaginary.

Consequently, this condition infers that the two roots of the equation must be real and negative.

$$\lambda_{\pm} = \frac{-\alpha \pm \sqrt{\alpha^2 - 4\beta}}{2} \tag{4.15}$$

We will check stability of Lagrange points one by one by using above equation.

4.2.1 Case I

By taking $a = 0.65$, $b = 0.346753850$, $d_1 = -1$, $d_2 = 1.15394$ and Lagrange points
$L_1 = (0.0293876, 0.6624051)$,
$L_2 = (-0.029008, 0.5170578)$,
$L_3 = (-1.525739, 1.6424128)$,
$L_4 = (-1.110806, 0.5477592)$,
$L_5 = (0.571680, -0.205759)$.

We show the stability analysis for these five equilibrium points in the following table.

Lagrange Points	**Eigenvalues**	**Stability**
L_1	$\pm 9.64483,\ \ 6.8286i$	Unstable
L_2	$\pm 9.64034,\ \ 6.7843i$	Unstable
L_3	$\pm 1.97834,\ \ 1.7357i$	Unstable
L_4	$\pm 3.82918,\ \ \pm 2.91198i$	Unstable
L_5	$\pm(0.366439 + 0.975362),\ \ \pm(0.366439 - 0.975362)$	Unstable

TABLE 4.1: Stability Analysis of Case I

4.2.2 Case II

By taking $a = 0.725$, $b = 0.400305651$, $d_1 = -1$, $d_2 = 1.12531$ and Lagrange points are $L_1 = (-1.53907, 1.60903)$, $L_2 = (-0.104273, 0.760995)$, $L_3 = (-0.100634, 0.446179)$, $L_4 = (-1.098, 0.536571)$, $L_5 = (0.58444, -0.24208)$.

We present the stability analysis for these equilibrium points in the subsequent table.

Lagrange Points	**Eigenvalues**	**Stability**
L_1	$\pm 1.94544,\ \ \pm 1.71513i$	Unstable
L_2	$\pm 5.57918,\ \ \pm 3.95147i$	Unstable
L_3	$\pm 5.42982,\ \ \pm 3.70414i$	Unstable
L_4	$\pm 4.36222,\ \ \pm 3.1832i$	Unstable
L_5	$\pm(0.382569 + 0.973369i),\ \ \pm(0.3825690.973369i)$	Unstable

TABLE 4.2: Stability Analysis of Case II

4.2.3 Case III

By taking $a = 0.8$, $b = 0.3467538$, $d_1 = -1$, $d_2 = 1.14675$ and Lagrange points are $L_1 = (-1.52971,\ 1.63825)$, $L_2 = (-0.148893,\ 0.851606)$, $L_3 = (-0.148112,\ 0.407786)$, $L_4 = (0.594372, -0.283447i)$, $L_5 = (-1.10005, 0.545286i)$.

We present the stability analysis for these five equilibrium points in the table below.

Lagrange Points	**Eigenvalues**	**Stability**
L_1	± 1.95688 , $\pm 1.72302i$	Unstable
L_2	± 4.9296, $\pm 3.50219i$	Unstable
L_3	± 4.64516, $\pm 3.13939i$	Unstable
L_4	$\pm(0.396808 + 0.970138i)$, $\pm(0.396808 - 0.970138i)$	Unstable
L_5	± 4.22751, $\pm 3.0865i$	Unstable

TABLE 4.3: Stability Analysis of Case III

4.2.4 Case IV

By taking $a = 0.95$, $b = 0.157594$, $d_1 = 1.05$, $d_2 = 0.13$ and Lagrange points are $L_1 = (0.886949, -0.325400)$, $L_2 = (-0.301525, -0.048973)$, $L_3 = (-1.019374, 0.390085)$, $L_4 = (-1.732356, 1.1718495)$, $L_5 = (-0.325802, 0.913011)$. We provide the stability analysis for these five equilibrium points in the table presented below.

Lagrange Points	**Eigenvalues**	**Stability**
L_1	± 2.8539, $\pm 2.13723i$	Unstable
L_2	± 14.1782, $\pm 9.83428i$	Unstable
L_3	± 7.7969, $\pm 5.1476i$	Unstable
L_4	± 1.95006, $\pm 1.64622i$	Unstable
L_5	± 13.7445, $\pm 9.57261i$	Unstable

TABLE 4.4: Stability Analysis of Case IV

We have tested equilibrium points for four cases and found all of them are unstable.

Chapter 5

Conclusion

In this research thesis, we reviewed the research work presented by Shoaib et al.[30]. The authors addressed the problem of finding the central configuration of four different coplanar masses and identified various symmetrical and non-symmetrical subsets of the four-body problem's central configuration.

In the extension work, we introduced a secondary mass and focused on studying the movement of a small mass (m_5) in the xy-plane, influenced by gravitational forces from four primary masses m_1, m_2, m_3, and m_4. By fixing the positions of the masses, the isosceles trapezoid central configuration established. We derived the equation of motion for (m_5), considering its negligible mass and minimal impact on the primaries. Subsequently, we fixed the positions of the primaries according to the established central configuration and calculated equilibrium points for m_5 across the interval of (a, b) within the fixed central configuration.

Additionally, we employed the multivariate Newton-Raphson iterative method to investigate convergence basins towards equilibrium points of the system. Plotting these basins of attraction in the xy-plane re-vealed significant variations in shape, nature, and the number of equilibrium points with changes in primary positions. Finally, we conducted stability analysis of all equilibrium points in the four cases.

Bibliography

[1] B. Steves and A. Roy, "Some special restricted four-body problems—i. modelling the caledonian problem," *Planetary and space science*, vol. 46, no. 11-12, pp. 1465–1474, 1998.

[2] K. R. Meyer and D. S. Schmidt, "Elliptic relative equilibria in the n-body problem," *Journal of Differential Equations*, vol. 214, no. 2, pp. 256–298, 2005.

[3] A. Albouy, Y. Fu, and S. Sun, "Symmetry of planar four-body convex central configurations," *Proceedings of the Royal Society A: Mathematical, Physical and Engineering Sciences*, vol. 464, no. 2093, pp. 1355–1365, 2008.

[4] J. Waldvogel, "The rhomboidal symmetric four-body problem," *Celestial Mechanics and Dynamical Astronomy*, vol. 113, pp. 113–123, 2012.

[5] B. Érdi and Z. Czirják, "Central configurations of four bodies with an axis of symmetry," *Celestial Mechanics and Dynamical Astronomy*, vol. 125, pp. 33–70, 2016.

[6] M. Shoaib, A. R. Kashif, and I. Szücs-Csillik, "On the planar central configurations of rhomboidal and triangular four-and five-body problems," *Astrophysics and Space Science*, vol. 362, no. 10, p. 182, 2017.

[7] M. Corbera, J. M. Cors, and G. E. Roberts, "A four-body convex central configuration with perpendicular diagonals is necessarily a kite," *Qualitative theory of dynamical systems*, vol. 17, pp. 367–374, 2018.

[8] M. Álvarez-Ramírez and J. Llibre, "Hjelmslev quadrilateral central configurations," *Physics Letters A*, vol. 383, no. 2-3, pp. 103–109, 2019.

[9] L. F. Mello and A. C. Fernandes, "Co-circular and co-spherical kite central configurations," *Qualitative theory of dynamical systems*, vol. 10, pp. 29–41, 2011.

[10] J. Bernat, J. Llibre, and E. Perez-Chavela, "On the planar central configurations of the 4-body problem with three equal masses," *preprint*, vol. 1, pp. 105–112, 2009.

[11] M. Santoprete, "Four-body central configurations with one pair of opposite sides parallel," *Journal of Mathematical Analysis and Applications*, vol. 464, no. 1, pp. 421–434, 2018.

[12] M. Celli, "The central configurations of four masses x,- x, y,- y," *Journal of Differential Equations*, vol. 235, no. 2, pp. 668–682, 2007.

[13] M. Corbera and J. Llibre, "Central configurations of the 4-body problem with masses $m_1 = m_2 > m_3 = m_4 =$ m> 0 and m small," *Applied Mathematics and Computation*, vol. 246, pp. 121–147, 2014.

[14] Z. Xia, "Convex central configurations for the n-body problem," *Journal of Differential Equations*, vol. 200, no. 2, pp. 185–190, 2004.

[15] M. Corbera, J. M. Cors, J. Llibre, and E. Pérez-Chavela, "Trapezoid central configurations," *Applied Mathematics and Computation*, vol. 346, pp. 127–142, 2019.

[16] J. M. Cors and G. E. Roberts, "Four-body co-circular central configurations," *Nonlinearity*, vol. 25, no. 2, p. 343, 2012.

[17] J. Gomez, A. Gutierrez, J. Little, R. Pelayo, and J. Robert, "Cocircular relative equilibria of four vortices," *Involve, a Journal of Mathematics*, vol. 9, no. 3, pp. 395–410, 2016.

[18] W. MacMillan and W. Bartky, "Permanent configurations in the problem of four bodies," *Transactions of the American Mathematical Society*, vol. 34, no. 4, pp. 838–875, 1932.

[19] F. R. Moulton, "On a class of particular solutions of the problem of four bodies," *Transactions of the American Mathematical Society*, vol. 1, no. 1, pp. 17–29, 1900.

[20] C. Simo, "Relative equilibrium solutions in the four body problem," *Celestial Mechanics*, vol. 18, no. 2, pp. 165–184, 1978.

[21] L. Bakker and S. Simmons, "A separating surface for sitnikov-like n+ 1-body problems," *Journal of Differential Equations*, vol. 258, no. 9, pp. 3063–3087, 2015.

[22] J. Wang, J.-Y. Yang, I. M. Fazal, N. Ahmed, Y. Yan, H. Huang, Y. Ren, Y. Yue, S. Dolinar, M. Tur, *et al.*, "Terabit free-space data transmission employing orbital angular momentum multiplexing," *Nature photonics*, vol. 6, no. 7, pp. 488–496, 2012.

[23] P. Rodgers, *Nanoscience and technology: a collection of reviews from nature journals*. World Scientific, 2009.

[24] W. L. Hamilton, J. Leskovec, and D. Jurafsky, "Diachronic word embeddings reveal statistical laws of semantic change," *arXiv preprint arXiv:1605.09096*, 2016.

[25] E. E. Zotos, "Fractal basins of attraction in the planar circular restricted three-body problem with oblateness and radiation pressure," *Astrophysics and Space Science*, vol. 361, no. 6, p. 181, 2016.

[26] M. S. Suraj, E. I. Abouelmagd, R. Aggarwal, and A. Mittal, "The analysis of restricted five–body problem within frame of variable mass," *New Astronomy*, vol. 70, pp. 12–21, 2019.

[27] E. E. Zotos and M. Sanam Suraj, "Basins of attraction of equilibrium points in the planar circular restricted five-body problem," *Astrophysics and Space Science*, vol. 363, pp. 1–16, 2018.

[28] B. I. Epureanu and H. S. Greenside, "Fractal basins of attraction associated with a damped newton's method," *SIAM review*, pp. 102–109, 1998.

[29] M. S. Suraj, P. Sachan, E. E. Zotos, A. Mittal, and R. Aggarwal, "On the newton-raphson basins of convergence associated with the libration points in the axisymmetric five-body problem: the concave configuration," *arXiv preprint arXiv:1904.04618*, 2019.

[30] M. Shoaib, B. Benhammouda, B. A. Steves, and W. L. Sweatman, "Central configurations in the general four body coplanar problem with different masses," 2023.

[31] M. R. Spiegel and Y. Proykova, "Schaum's outline of theory and problems of theoretical mechanics: with an introduction to lagrange's equations and hamiltonian theory," 1967.

[32] S. Alrasheed, *Principles of mechanics: Fundamental university physics*. Springer Nature, 2019.

[33] A. E. Roy, *Orbital motion*. CRC Press, 2020.

[34] W. H. Goodyear, "Completely general closed-form solution for coordinates and partial derivative of the two-body problem," *Astronomical Journal, Vol. 70, p. 189*, vol. 70, p. 189, 1965.

[35] R. Fitzpatrick, *An introduction to celestial mechanics*. Cambridge University Press, 2012.

[36] R. Moeckel, "Central configurations," *Central Configurations, Periodic Orbits, and Hamiltonian Systems, Adv. Courses Math. CRM Barcelona, Birkhäuser/Springer, Basel*, pp. 105–167, 2015.

[37] A. Celletti *et al.*, "Celestial mechanics: from antiquity to modern times," in *Celestial Mechanics*, EOLSS-UNESCO publ., 2015.

[38] M. Gidea and J. Llibre, "Symmetric planar central configurations of five bodies: Euler plus two," *Celestial Mechanics and Dynamical Astronomy*, vol. 106, pp. 89–107, 2010.

[39] M. Siddique, A. Kahsif, M. Shoaib, and S. Hussain, "Stability analysis of the rhomboidal restricted six-body problem," *Advances in Astronomy*, vol. 2021, pp. 1–15, 2021.